Kaunas University of Technology

Faculty of Electrical and Electronics Engineering

Development and Investigation of Biomass Growth Adaptive Control System in Bioreactor of Fed-Batch Operating Mode

Master's Final Degree Project

Sandesh Mysore Sathyaraj

Project author

Prof. Dr. Donatas Levišauskas

Supervisor

Kaunas, 2019

Kaunas University of Technology

Faculty of Electrical and Electronics Engineering

Development and Investigation of Biomass Growth Adaptive Control System in Bioreactor of Fed-Batch Operating Mode

Master's Final Degree Project

Control Technologies (6211EX014)

Sandesh Mysore Sathyaraj

Project author

Prof. Dr. Donatas Levišauskas

Supervisor

Doc.Dr. Renaldas Urniežius

Reviewer

Kaunas, 2019

Kaunas University of Technology

Faculty of Electrical and Electronics Engineering

Sandesh Mysore Sathyaraj

Development and Investigation of Biomass Growth Adaptive Control System in Bioreactor of Fed-Batch Operating Mode

Declaration of Academic Integrity

I confirm that the final project of mine, Sandesh Mysore Sathyaraj, on the topic „Development and Investigation of Biomass Growth Adaptive Control System in Bioreactor of Fed-Batch Operating Mode "is written completely by myself; all the provided data and research results are correct and have been obtained honestly. None of the parts of this thesis has been plagiarized from any printed, Internet-based or otherwise recorded sources. All direct and indirect quotations from external resources are indicated in the list of references. No monetary funds (unless required by Law) have been paid to anyone for any contribution to this project.

I fully and completely understand that any discovery of any manifestations/case/facts of dishonesty inevitably results in me incurring a penalty according to the procedure(s) effective at Kaunas University of Technology.

(name and surname filled in by hand)	(signature)

Sandesh Mysore Sathyaraj. Biomasės augimo adaptacinės kontrolės sistemos sukūrimas ir tyrimas Fed-Batch veikimo režimo bioreaktoriuje. Valdymo sistemu magisto baigiamasis projektas / vadovas prof, dr, Donatas Levisauskas; Kauno technologijos universitetas, Elektros ir elektronikos fakultetas, Automatikos katedra.

Mokslo kryptis ir sritis: Elektronikos inžinerija, Inžinerijos mokslai

Raktiniai žodžiai: įgyti nuskaitymą, PID reguliatorių, reguliatorių, modeliavimą, prisitaikymą.

Kaunas, 2019.55 p.

SANTRAUKA

Šiame darbe aprašoma glicerolio kontrolės sistema. Išnagrinėtas glicerolio kontrolės sistemos veikimas ir nustatyti faktiniai intervalai.

Tyrimo dalyje aprašomi tyrimo metodai: Pirmosios eilės laiko atidėjimo modeliai, antrosios eilės polinomo modelis, PID valdymo algoritmas, Cohen ir Coon derinimo taisyklės.

Tyrimo tiriamojoje dalyje skaičiavimai atlikti pagal tris skirtingus metodus. Matematiniai modelio parametrai gaunami naudojant atvirojo kontūro testą. Apskaičiuoti reakcijos kreivės rezultatai palyginami su eksperimentiniais rezultatais, naudojant antrosios eilės polinomo metodą. Eksperimentiniai rezultatai buvo atlikti naudojant adaptyvią sistemą ir ne adaptyvius sistemos metodus. Palyginti abiejų metodų rezultatai ir išspręsta problema. Pateiktos skaičiavimo lentelės su rezultatais ir optimizuotais rezultatų grafikais.

Eksperimentiniai skaičiavimai, programavimas ir modeliavimas atliekamas naudojant MATLAB / SIMULINK programinę įrangą.

Sandesh Mysore Sathyaraj. Development and Investigation of Biomass Growth Adaptive Control System in Bioreactor of Fed-Batch Operating Mode. Title of the Final Degree Project control systems Master's Final Degree Project/supervisor Assoc. prof. Donatas Levišauskas. Kaunas University of Technology, Faculty of Electrical and Electronics Engineering, Department of automation.

Study field and area (study field group): Electronics Engineering, Engineering Sciences.

Keywords: gain scheduling, PID controller, regulator, modelling, adaptive.

Kaunas, 2019.55 p.

SUMMARY

This work describes the glycerol control system. The operation of the glycerol control system has been analyzed and actual showing intervals determined.

The research part describes the research methods: First order time delay models, second order polynomial model, PID control algorithm, Cohen and Coon tuning rules.

In the investigation part of the study, the calculation was made according to three different methods. The mathematical model parameters are obtained using an open loop test. The calculated reaction curve results are compared with experimental results using a second order polynomial method. The experimental results were carried out using an adaptive system and non-adaptive system methods. The results of the two methods were compared and the problem was solved. The tables of calculation with the results and the optimized results graphs are presented.

Experimental calculations, programming and modelling performed using MATLAB/SIMULINK software.

Table of Contents

LIST OF ABBREVIATION AND TERMS

ACS- Adaptive Control System

SGR(μ)- Specific Growth Rate;

OUR-Oxygen Uptake Rate;

K-Gain coefficient;

T-Time constant;

τ-Time delay;

Kc-Proportional gain;

Ti-Integration time constant;

Td-Differentiation time constant;

DEE- Differentiation equation editor block;

u-Feeding rate;

V-Volume broth;

x-Biomass concentration;

s-Substrate concentration;

μ_{set}-Set-point value of μ;

NASA-National Aeronautics and Space Administration;

BPS-Biomass Production System.

t_k-time moment at k

INTRODUCTION

1. INTRODUCTION TO CONTROL TECHNOLOGY

Initially, some universal characteristics of bioreactors are highlighted with reference to control applications. Two main features, it is important to know before designing a control system for bioreactors, are:

- The multivariable system, and
- Non-linear dynamics.

The control of a bioreactor comprises many variables. Device measurement and control technologies applied to a standard bioreactor are well known in classical process engineering [1].

1.1. Control system

In recent years, control systems have played a central role in improving and advancing current technology and civilization. Practically each one of the subjects of our daily life is affected with the help of some system of manipulation. A bathroom, a tank, a refrigerator, an air conditioner, an ironing machine, a computerized iron, a vehicle, everything is a control system [2][1].

1.1.1. Open loop control systems

Any physical system without any automatic correction of variation towards the output change which is called an open loop control system. This type of systems is simple to construct, stable and cheap but it will not maintain its accuracy and reliability. These systems do not have external disturbance to affect the output and it will not initiate correction action automatically [2].

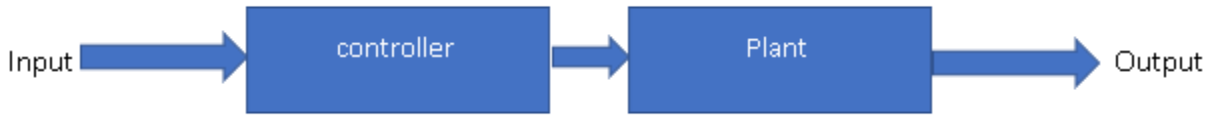

Figure 1. Block diagram of the open-loop control system [2]

1.1.2. Closed loop control systems

A closed loop control system is a system will maintain desired output values in accordance with input quantity in a closed loop manner, as shown in Figure 2. This type of systems is complicated to construct as compared to an open loop system [2].

1.1.3. Biomass Growth Control System

In collaboration with NASA under the SBIR (Small Business Innovation Research) program, it is established by orbital technologies corporation to meet the growing needs of commercial, biotechnology and science plants in the era of the Space Station. The BPS was developed based on interactions with NASA engineers and scientists and on the "lessons learned" from already flown plant growth systems, including the ASTROCULTURETM unit, Plant Growth Plant and Bio-processing Apparatus of plants [3].

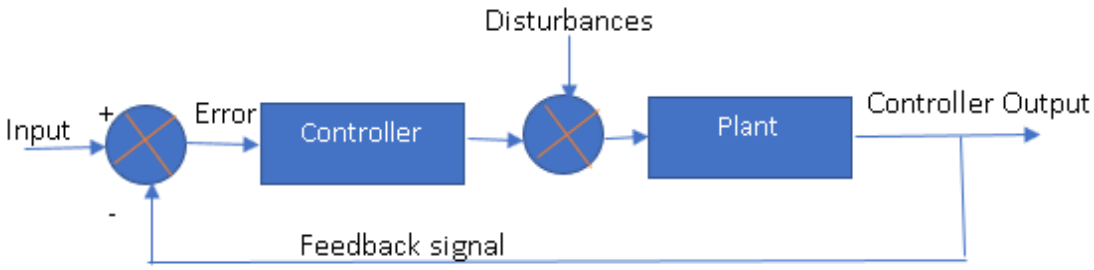

Figure 2. Block diagram of closed loop control systems [2]

1.2. Types of bioreactors or fermenters

A biological reaction carried out into a vessel and culture aerobic cells are used for conducting enzymatic immobilization [4]. Different types of bio-reactor or fermenters: Continuous Stirred Tank Bioreactor**:** In a vessel, the time will no longer vary the contents to hold up of micro-organisms and the components will contain some concentration in the fermenter. To achieve steady-state conditions by chemo static principles. These types of bioreactor are commonly used in a continuous process to activate in wastewater sludge industry. Airlift Bioreactor**:** The capacity, kinetic data, the specific growth rate is determined from rector volume of the organism used. The airlift pump works on a principle of fermenter are internal loop type and external loop type respectively. The uniform cylindrical cross type and has a configuration of the internal and external loop.Fluidized Bed Bioreactor: The regular particles contain some characteristics that are suspended in a flowing liquid stream with some additional gas phase is involved in this bioreactor, the tendency of particles which are involved in the bed that is less evenly distributed.Photo Bioreactor: Phototrophic microorganism is used with some light source to cultivate. The photosynthesis is used by organisms to trigger biomass from the light source and carbon dioxide. The respective species are controlled for the artificial environment of a photobioreactor. In the photobioreactor, growth rate and level of purity in nature will be higher other than anywhere. Membrane Bioreactor: The various microbial bioconversions are applied successfully by membrane bioreactor. The alcoholic fermentation, solvents, organic acid production, wastewater treatment used in microbial conversions. The soluble enzyme and substrate are used in membrane bioreactor on one side of the ultrafilter membrane [5].

1.3. The operating modes of bioreactor

In a bioreactor, all the bioprocesses are carried out, where a microorganism like bacteria, fungi, yeast is cultivated under product formation conditions. For this reason, nutrients are compulsorily required to grow and under some conditions like temperature, pressure, PH and oxygen concentration are required to control the microorganism and these are the basic requirements to control bioprocess in a bioreactor [6].Batch mode, in this mode no substrate is added to the initial charge and no product is taken until it finishes the process. In batch operation have a major advantage for low investment cost, it does not require much control and without skilled labor, it can be accomplished operation. It has greater flexibility can be accomplished by using a bioreactor in various fields of product [6]. Fed-batch mode, in this mode during operation substrates are fed into the bioreactor. The combination of the batch and continuous operation are very popular in the ethanol industry. It has the main advantage is that inhibition and catabolite repression are avoided and additionally improves the productivity of the broth by holding at a low substrate concentration [6]. The continuous mode in this mode the

substrate is added continuously until it finishes the process and product removal. In this process, the product is taken from the top of the bioreactor such as ethanol, cells and residual sugar as shown in Figure 3. Here operation is classified into two types, single stage continuous fermentation and multi-stage continuous fermentation [6]. The research part describes the research methods, first order time delay models, second order polynomial model, PID control algorithm, Cohen and Coon tuning rules Experimental calculations, programming and modelling performed using MATLAB/SIMULINK software.

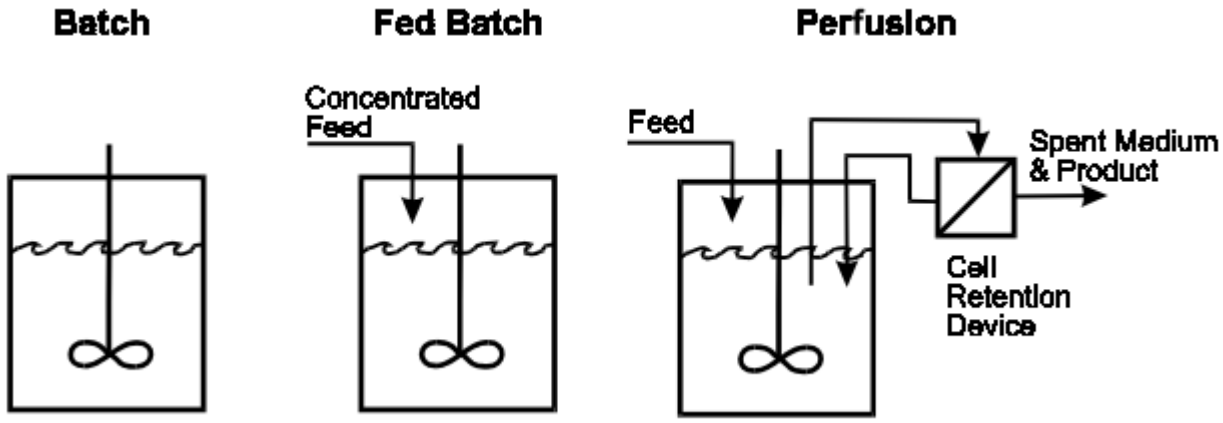

Figure 3. Alternate stirred bioreactor processes [7]

AIM: To develop and investigate biomass growth control system in fed-batch operating mode bioreactor.

TASKS: To develop and investigate a model for simulation of adaptive control system performance for tracking of specific growth rate at specific setpoint time trajectories and compare the result with ordinary control system performance indices.

2. LITERATURE REVIEW

In microbiology, researchers often faced problems in describing the growth-rate of microorganisms growing on sub-strategy or in the study of competition through depletion resource. Improved growth rate and growth function from a mathematical model of flocs and microbial using negative feedback density-dependent process Compared growth rate and cell size in homeostasis at the metabolic signal in the cell division according to animal cell [8][9].Obtained biofilm growth from purple non-sulfur bacteria using a mathematical model of photo-bioreactor. The synthesis, design, and decision making related to the wastewater treatment process modelling Measured leaf chlorophyll from biomass production under various heat stress treatments during climate change occur in critical wheat production [10] [11]. Developed leaf elongation and leaf appearance derived from maize production during crop modelling and climate change condition [13].

Identified heat stress and grain filling in leaf chlorophyll of photosynthesis during leaf area index dynamics are carried in climate change for wheat production. The Wheat Grow model is a process-based wheat model, which can predict wheat phenology, photosynthesis and biomass production, biomass partitioning and organ establishment, and grain yield and quality formation under various environmental factors and management practices [10]. Compared to large cells and small cells are achieved multiple signaling pathways in cell division of growth rate and cell cycle progression helps to find in homeostasis [8]. Indicated unidentified extracellular components from bacteria will increase biomass and lipid productivities in a co-cultivation of algae and will reduce the expenditure in mass algae cultivation process in microorganisms [12].

2.1. Mathematical modelling of Fed-batch fermentation

Maximized enzyme activity by reducing metabolic heat and feeding inlet air in solid-state fermentation of a fixed bed reactor [14]. Developed excessive lovastatin 3.5-fold by microparticles of the preculture during bioreactor process [15]. Improved simultaneously high solids of saccharification and fermentation by recycle membrane from paper production of lactic acid [16]. The developed dynamic model for metabolic pathway in a sequential identification method [17]. Modified ethanol production at different temperature in the production of wine using yeast hinder [18]. Removed aerobic oxide of biomass segmentation with ammonium-oxidizing and nitrite-oxidizing impact on microbial [19]. Developed growth and decline phase of specific growth rate and biomass estimation in penicillin production of microorganisms [20]. Integrated model computation and biomass model of NIR data applied control overflow metabolism using partial least square and control a cholera-toxin in the monitor of batch cultivation [21]. Obtained numerical simulation of substrate feed rate in batch-to-batch process and leads to a robust process from measured problems in protein production [22]. Showed that heat capacity calorimeter of growth behavior will help to find validity and accuracy in a fermentation process used in many applications by this simple strategy [23]. Evidenced that glycan fractions with a heavy chain and the protein abundance enzyme to measure the time evolution of heterogeneities in pharmaceutical production as shown in Figure 4 [24][25]. Solved multi-objective optimization in a significant way the feed recipe helps to create productivity from dynamic optimization problems [26]. Showed the strain stability in ABE concentrations carried from oxygen tolerant process enforced by a butanol and acetate production [27]. Introduced multi-objective optimization in a distinct objective is computed to optimum algorithms for the productivity of dynamic optimization problems [26]. Observed enzyme activity of monoclonal antibodies in a bioreactor scale to improve intracellular clustering of micro-

heterogeneities mining method for an absolute measure of scale in a pharmaceutical production [25]. Compared heat capacity calorimetry to compensation mode in a validity and accuracy, since mainly deal with PAT solution [23]. Analyzed the NIR data and EN data in partial least square with high correlation biomass, glucose, and acetate during monitoring and control of spectral identification [21]. Estimated the growth and decline phase for the development of control strategy in specific growth rate via online estimation method for specific production in penicillin production of bioprocess filamentous microorganisms to control quantitative and qualitative process [20].

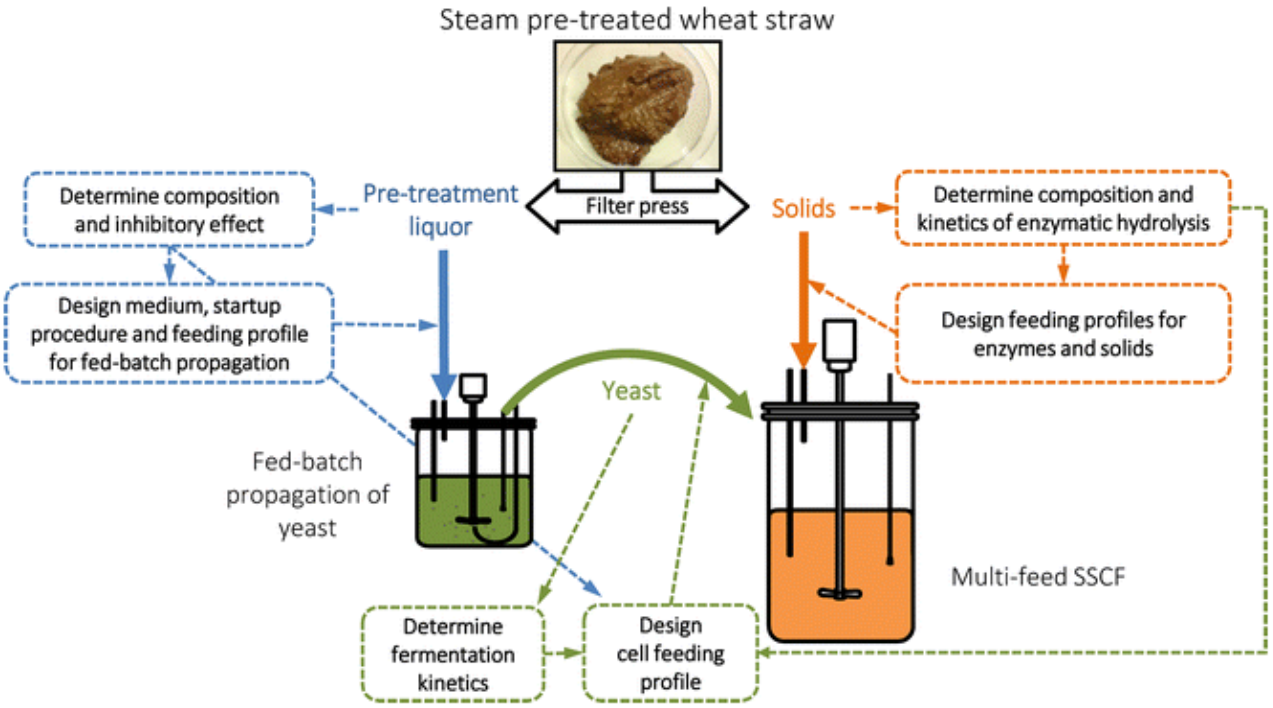

Figure 4. Process optimization [24]

2.2. Adaptive control system applied for biomass growth control in fed-batch cultivation processes

The oxygen concentration in the exhaust gas and the air supply rate no need of a mathematical model for the culture of microorganisms under control using fed-batch cultivation process having inferential control algorithm [28]. The recombinant production systems for collecting the data straight forward by controlling experiments for optimization predefined specific growth rate of the green fluorescent protein for keeping a microbial cultivation process in a generic control model [29].In simulation experiment fast adaptation, robust behavior significant changes in control performance for controlling dissolved oxygen concentration into control algorithm of steady-state action for adaptation controller to process on-linearity and time-varying operating conditions of microbial process [30].The transient response and robustness sliding observer an estimation growth rate it is implemented to control law using Lyapunov functions feed-back proportional output error for nonlinear integral action of the biomass specific growth rate based on the minimal model paradigm. The yeast Saccharomyces cerevisiae in glucose-limited chemostat culture indeed the affinity of the enzyme its transport on the specific growth rate for its growth-limiting substrate [31].The recombinant proteins are produced more in the robust process which is reliable, fast for various monitoring techniques of the specific growth rate in the microbial fed-batch mode for real-time estimation and other measurable variables

to grow the microorganisms essential in product quality [32]. The fermentation of glucose and acetate developed observer, estimator and controller in E.coli fed-batch fermentation desired recombinant protein for a specific growth rate it often related simulations by characterizing microorganisms [33]. Online regulation is usually limited to maintaining a small number of environmental conditions such as broth temperature, pH and dissolved oxygen level.

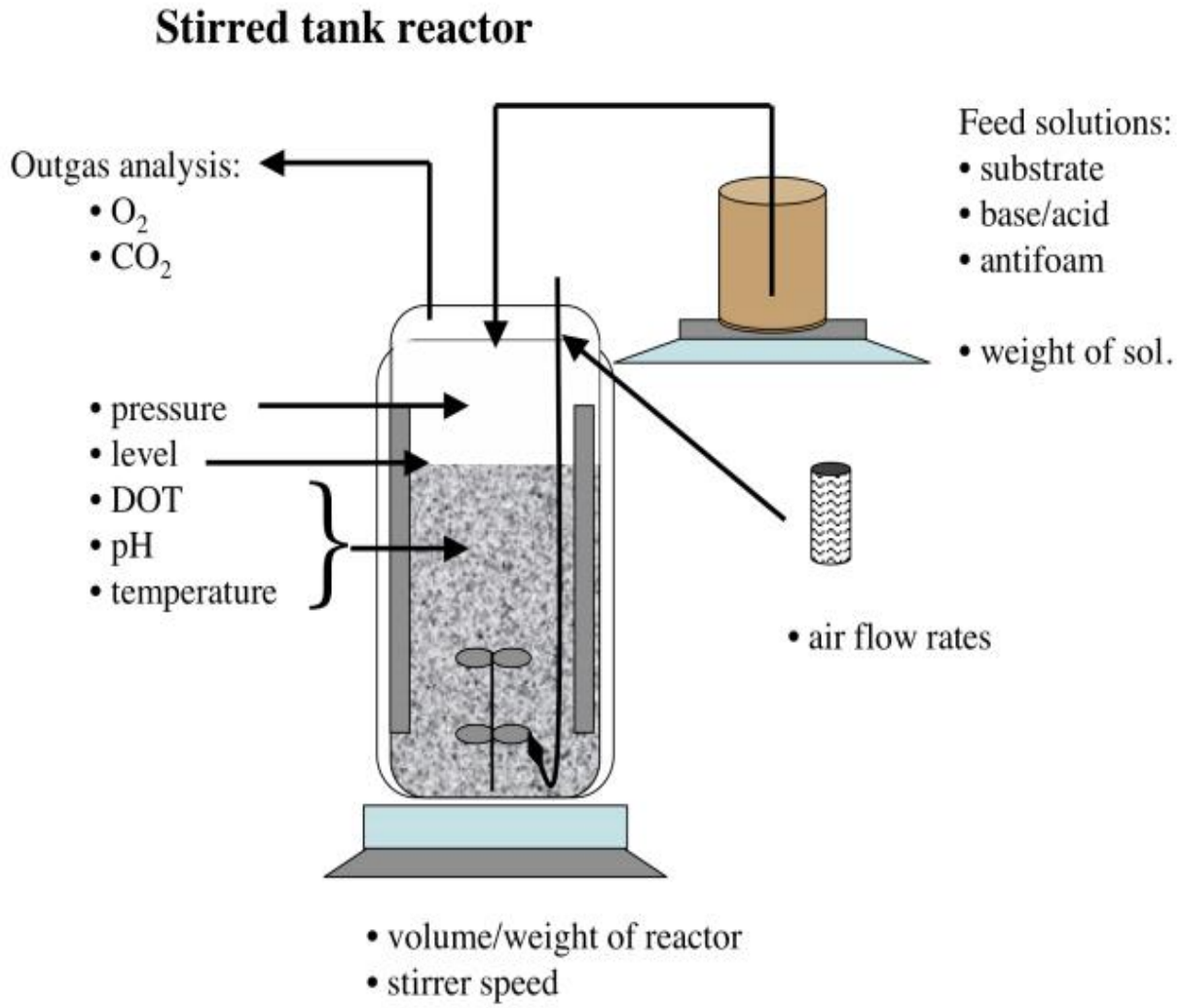

Figure 5. Instrumentation and monitoring of bioreactor [34]

Fermentation processes can also have a classical problem associated with interactions between multiple variable systems, which help complicate regulator regulation. The controller is usually tuned by loop loops, ignoring the effects of any process interactions. A trajectory of the benchmark that optimizes fermentation is difficult to specify and a more in-depth approach to specifications should be developed as shown in Figure 5 [34].

3. DEVELOPMENT OF ADAPTIVE CONTROL SYSTEMS

The modelling of the modelled data management system structure is shown in Figure 6 an experimental research idea and experimental design of the subject was created. Based on polynomial results of gain coefficient(k), a time constant(T) and time delay (Tau) were evaluated, next moving to experimental results using the least square method. For example, the polynomial model of the process parameter was created, and the ACS model was created using the MATLAB/SIMULINK software tool. By modifying the control law adaptive system works slowly the time changes of any parameters of a specific system. ACS motivated to improve the performance of the fixed gain control system. The adaptive control can have less dependent to the accuracy of the mathematical models of the system, but fixed gain controller mainly relies on it, since there will be no variation in the system dynamics [35](appendix Number 14).

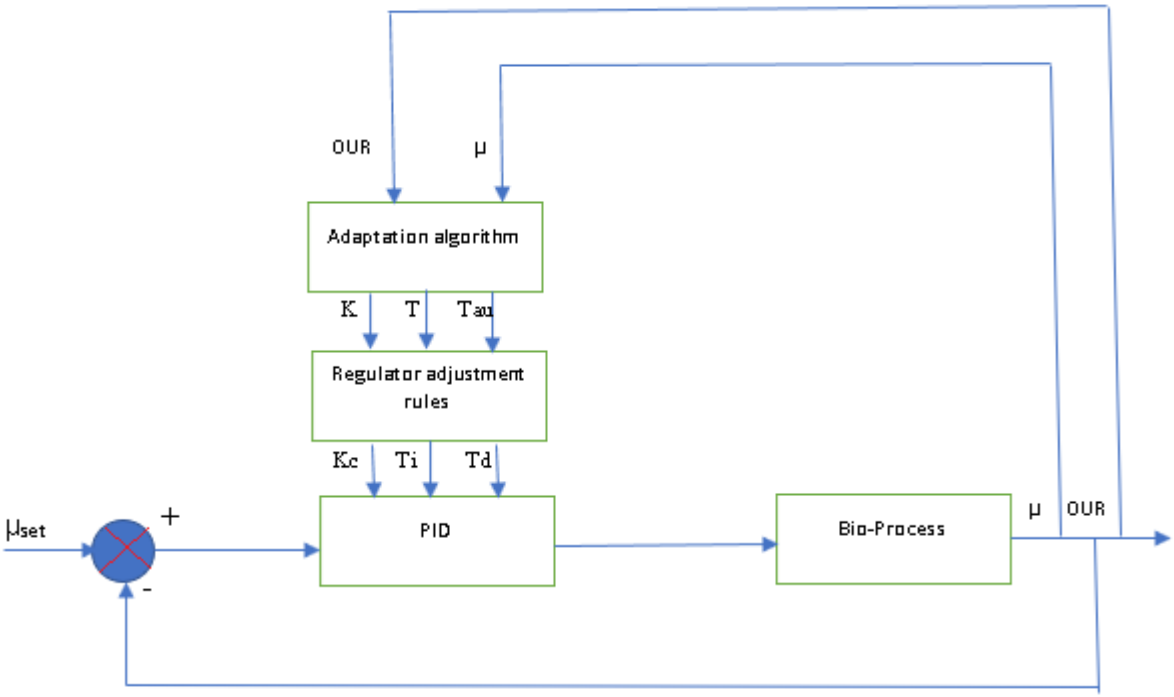

Figure 6. Block scheme of ACS [35]

The dynamic parameters of the system consist of the oxygen uptake rate(OUR) and the growing of specific growth rate(μ) for glycerol. In this parameter, the gain coefficient(k), time constant(T) and time delay(τ) is determined. The Cohen and Coon method (Smith method) is provided for tuning of the controller parameters. In both cases, the PID regulator's parameter remains the same as the algorithm for the regulatory variation. The differential parameter is integrated into the DEE block at the control object. General different models for modelling of specific growth rate formulae as shown in Table 1.

Table 1. Typical models for modelling of specific growth rate [34][35][36]

SL NO	Specific Growth Rate (SGR) (Model Equation)	Authors	Comments
1	μ = Constant	-	-
2	μ = KS	-	-

3	$\mu = KS^n$	-	-
4	$\mu = \frac{\mu msk}{ks+s}$	Monod function	Empirically derived from the Michaelis and Menten equation
5	$\mu=\frac{(\mu m(1+s/k1)}{(1+s/k2))}$	Haldane/Andrews function	Substrate inhibition in a chemostat
6	$\mu =\frac{\mu ms}{ks+s+\frac{s2}{ki}}$	Webb function	-
7	$\mu =\frac{\mu ms\left(1+\frac{s}{ki}\right)}{(ks+s)\left(1+\frac{s}{ki}\right)}$	Andrews function	Substrate inhibition in a chemostat
8	$\mu =\frac{\mu max\ ((sn\ /ks))}{sn}$	Moser	Analog with hill kinetics(n>0)
9	$\mu =\frac{\mu\ \max(1-e-s)}{kS}$	Tessier	-
10	$\mu =\frac{\mu msk}{(ks+s)e^{-\frac{s}{k_{i,S}}}}$	Aiba	-
11	$\mu(S)=\mu_{max}\frac{s}{k_s+k_D+s}$	Powell Equation	Influence of cell permeability, substrate diffusion and cell dimensions
12	$\mu(S) = \mu_{max}\ (1\text{-}k_sX)$	Verhulst	It is known as growth logical model
13	$\mu(X,S) = \mu_{max}\frac{s_0-\frac{x}{y}}{k_s+s_0-\frac{x}{y}}$	Meyrath	It is based on Monod kinetics
14	$\mu=\mu_{max}\frac{s}{k_xx+s}$	Contois	If S=constant, the only dependence remains μ = f(x)
15	$\mu = \mu_{max}\frac{1}{1+\frac{k_s}{S}+\sum_j\left(\frac{s}{k_{j,s}}\right)^j}$	Yano model	-
16	$\mu(P) = \mu_{max} - k_1(p-k_2)$	Holzberg	-
17	$\mu(P) = \mu_{max}(1-\frac{p}{p_{max}})$	Ghose and Tyagi	-

3.1. Mathematical model of the fed-batch cultivation process

Using a simple bioprocess model are controller initial first test was performed and E. coli growing on glycerol using fed-batch cultivation was simulated in the following way, mass balance equation of biomass concentration [36](appendix Number 1 and Number 2).

$$\frac{dx}{dt} = \mu x - u\frac{x}{V}. \quad (1)$$

Mass balance equation of substrate concentration [36]

$$\frac{ds}{dt} = -\frac{1}{Y_{xs}}\mu x - mx + u\frac{s_f - s}{V}. \quad (2)$$

Mass balance equation of specific growth rate(μ) [36]

$$\frac{d\mu}{dt} = \frac{1}{T}\left(\mu_{max}\frac{s}{K_s+s} * \frac{K_i}{K_i+s} - \mu\right). \quad (3)$$

Mass balance equation of volume fermentation broth [36]

$$\frac{dV}{dt} = u. \quad (4)$$

A wide class of fermentation process of oxygen uptake rate (OUR) [36]

$$OUR = \alpha\mu xV + \beta xV. \quad (5)$$

In simulation experiments the parameters values and initial conditions of the state variables as shown in the Table 2(appendix Number 1).

Table 2. Model parameter and initial condition of state variables [37]

Y_{XS}	0.8 gg^{-1}
M	0.02 $g(gh)^{-1}$
A	0.82 gg^{-1}
B	0.01 $g(gh)^{-1}$
μ_{max}	1.1 h^{-1}
K_s	0.7 gl^{-1}
K_i	85 gl^{-1}
s_f	150 gl^{-1}
x(0)	0.5 gl^{-1}
s(0)	5.0 gl^{-1}
V(0)	8.0 l

According to initial values and model parameters of state variables for specific growth rate values are taken from 0.1 - 0.6 h^{-1} with corresponding oxygen uptake rate (OUR) values are also noted down as per simulation time using open loop test (Smith method). This method helps to find basic dynamic parameters like Gain coefficient(k), Time constant(T), Time delay(τ) for analyzing further steps.

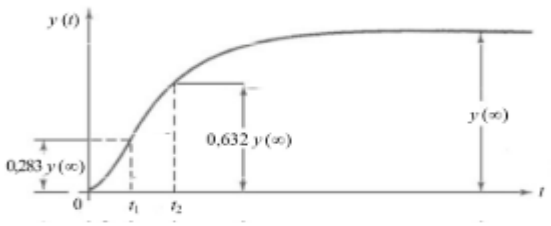

Figure 7. Estimating of parameter values of first order plus time delay process model [37]

In this method we are dealing with the process reaction curve by first order plus time delay model, then it is possible to obtain controller parameters from this curve shown in Figure 6 [37],

$$T_{pr} = \frac{3}{2}(t_2 - t_1) \quad (6)$$

$$\tau_{pr} = t_2 - T_{pr} \quad (7)$$

$$k_{pr} = \frac{y_{peak}}{\Delta u} \quad (8)$$

$$y(t_1) = 0.283y_{peak} \quad (9)$$

$$y(t_2) = 0.632y_{peak} \quad (10)$$

k_{pr} = gain coefficient

T_{pr} = time constant

τ_{pr} = time delay

y_{peak} = maximum peak value of the curve

These relationships are used empirically to provide a closed-loop response of the system and give a better result to process reaction curve. According to the above method, calculated parameters of gain coefficient(k), time constant(T), the time delay(τ) respectively. Approximation of specific growth rate response to a step change in feed rate by first order plus time delay model(appendix Number 3 and Number 4).

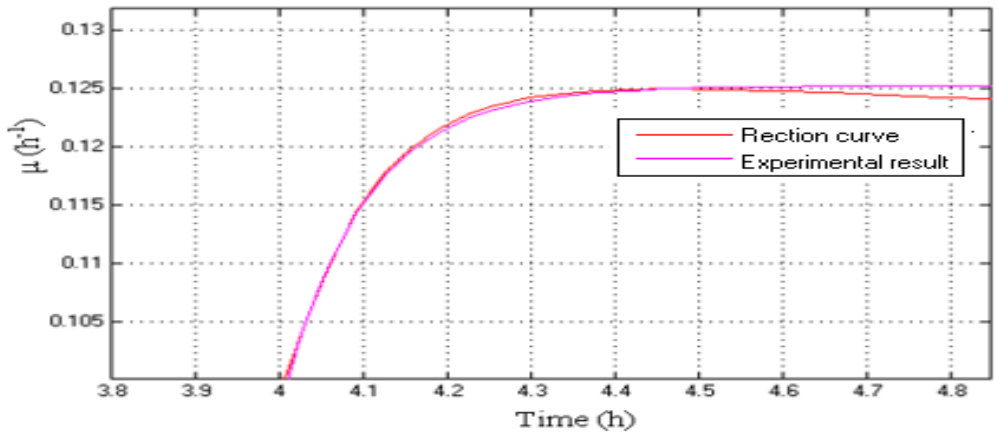

Figure 8. Simulation results of model-based specific growth rate response and its approximation by first order plus time delay model and estimated parameters values of first order plus time delay model are k=2.37, T=0.0957, τ=0.0099, μ=0.1.

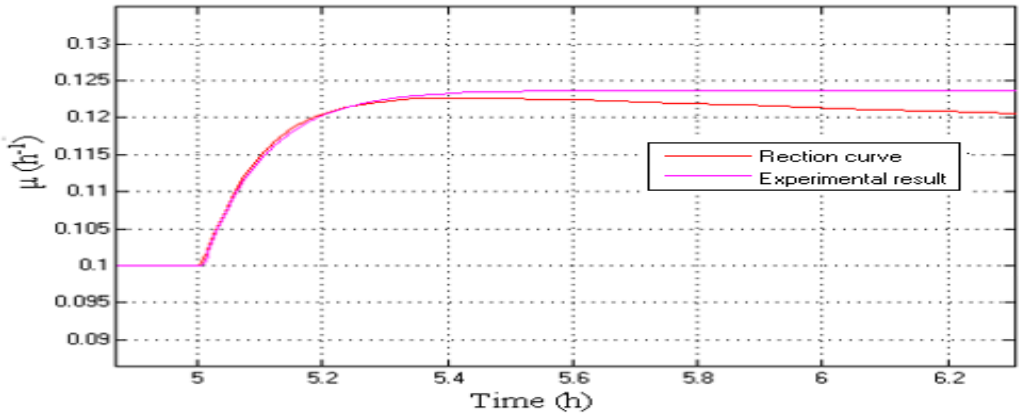

Figure 9. Simulation results of model-based specific growth rate response and its approximation by first order plus time delay model and estimated parameters values of first order plus time delay model are k=2.14, T=0.0869, τ=0.0095, μ=0.1.

As shown in Figure 8, the x-axis indicates the time(h) and the y-axis indicates a specific growth rate (μ) of 0.1. The simulation time starts at 4 (h) in which the red line shows the reaction curve in open loop test (Smith method) and the pink line shows the experimental result by using first order plus the time delay function and dynamic parameters values are calculated by this graph k=2.37, T=0.0957, τ=0.0099, μ=0.1 respectively. As shown in Figure 9, the x-axis indicates the time(h) and the y-axis indicates a specific growth rate (μ) of 0.1. The simulation time starts at 5 (h) in which the red line shows the reaction curve in open loop test (Smith method) and the pink line shows the experimental result by using first order plus the time delay function and dynamic parameters values are calculated by this graph k=2.14, T=0.0869, τ=0.0095, μ=0.1 respectively.

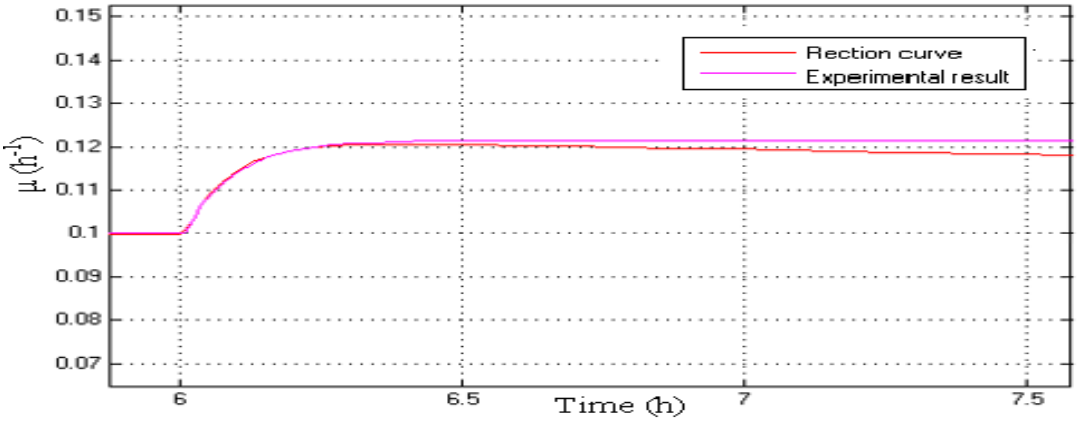

Figure 10. Simulation results of model-based specific growth rate response and its approximation by first order plus time delay model and estimated parameters values of first order plus time delay model are k=1.87, T=0.0689, τ=0.0087, μ=0.1.

As shown in Figure 10, the x-axis indicates the time(h) and the y-axis indicates a specific growth rate (μ) of 0.1. The simulation time starts at 6 (h) in which the red line shows the reaction curve in open loop test (Smith method) and the pink line shows the experimental result by using first order plus the time delay function and dynamic parameters values are calculated by this graph k=1.87, T=0.0689, τ=0.0087, μ=0.1 respectively.

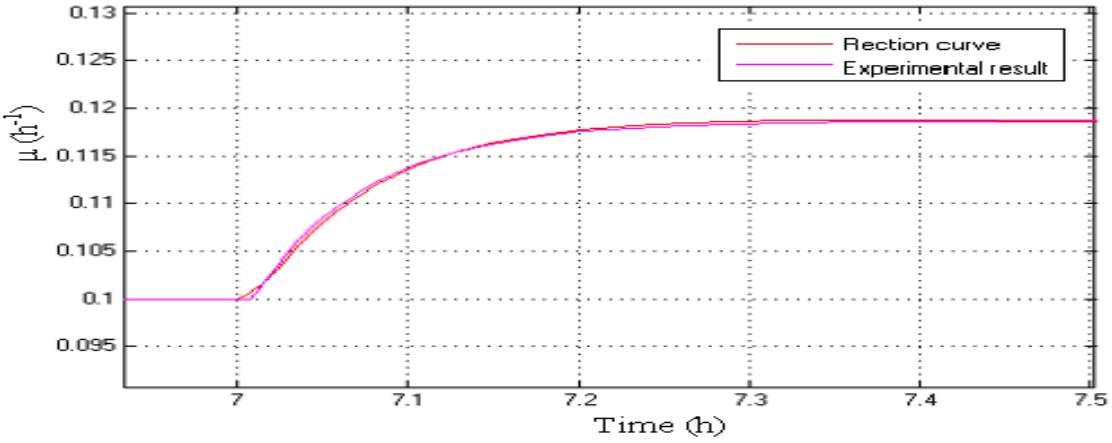

Figure 11. Simulation results of model-based specific growth rate response and its approximation by first order plus time delay model and estimated parameters values of first order plus time delay model are k=1.7, T=0.0627, τ=0.0077, μ=0.1.

As shown in Figure 11, the x-axis indicates the time(h) and the y-axis indicates a specific growth rate (μ) of 0.1. The simulation time starts at 7 (h) in which the red line shows the reaction curve in open loop test (Smith method) and the pink line shows the experimental result by using first order plus the time delay function and dynamic parameters values are calculated by this graph k=1.7, T=0.0627, τ=0.0077, μ=0.1 respectively.

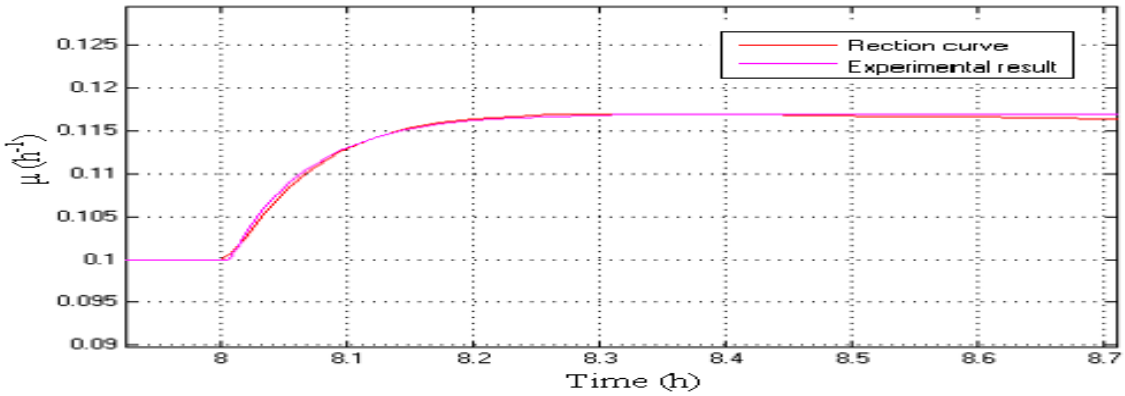

Figure 12. Simulation results of model-based specific growth rate response and its approximation by first order plus time delay model and estimated parameters values of first order plus time delay model are k=1.4, T=0.0510, τ=0.0066, μ=0.1.

As shown in Figure 12, the x-axis indicates the time(h) and the y-axis indicates a specific growth rate (μ) of 0.1. The simulation time starts at 8 (h) in which the red line shows the reaction curve in open loop test (Smith method) and the pink line shows the experimental result by using first order plus the time delay function and dynamic parameters values are calculated by this graph k=1.4, T=0.0510, τ=0.0066, μ=0.1 respectively.

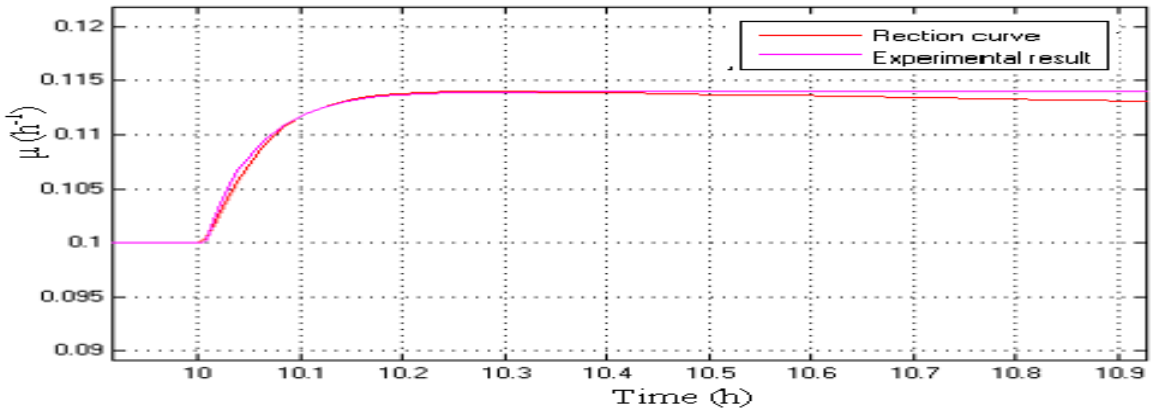

Figure 13. Simulation results of model-based specific growth rate response and its approximation by first order plus time delay model and estimated parameters values of first order plus time delay model are k=0.89, T=0.0408, τ=0.0056, μ=0.1

As shown in Figure 13, the x-axis indicates the time(h) and the y-axis indicates a specific growth rate (μ) of 0.1. The simulation time starts at 10 (h) in which the red line shows the reaction curve in open loop test (Smith method) and the pink line shows the experimental result by using first order plus the time delay function and dynamic parameters values are calculated by this graph k=0.89, T=0.0408, τ=0.0056, μ=0.1 respectively.

Table 3. First order plus time delay model parameters at various levels of oxygen uptake rate(OUR) and specific growth rate(SGR)

SL no	MU	OUR	K	T	TAU
1	0.1	4.6304	2.37	0.0975	0.0099
2	0.1	5.1194	2.14	0.0869	0.0095

3	0.1	5.6578	1.87	0.0689	0.0087
4	0.1	6.2529	1.7	0.0627	0.0077
5	0.1	7.6367	1.4	0.0510	0.0066
6	0.1	12.5927	0.89	0.0408	0.0056
7	0.2	12.1234	1.595	0.07395	0.01195
8	0.2	14.8081	1.32	0.06105	0.0115
9	0.2	18.0872	1.1	0.05085	0.01135
10	0.2	22.0922	0.905	0.0425	0.0108
11	0.2	32.9967	0.63	0.03125	0.0099
12	0.3	24.3869	1.1433	0.0681	0.0118
13	0.3	32.9233	0.8666	0.05265	0.01115
14	0.3	44.4447	0.65333	0.04095	0.01035
15	0.3	59.9968	0.49	0.0318	0.0102
16	0.3	109.0498	0.28	0.0234	0.0077
17	0.4	43.2441	0.8275	0.06705	0.01215
18	0.4	64.5238	0.575	0.04815	0.01125
19	0.4	96.2653	0.395	0.03525	0.01025
20	0.4	143.6018	0.28	0.0278	0.0092
21	0.5	71.0925	0.608	0.06975	0.01315
22	0.5	117.2368	0.386	0.04905	0.01145
23	0.5	193.3035	0.243	0.03375	0.01115
24	0.5	318.7199	0.155	0.02685	0.00915
25	0.6	110.0697	0.451	0.08085	0.01275
26	0.6	200.5792	0.2265	0.05325	0.01155
27	0.6	365.4866	0.161	0.0447	0.0081

Based on simulation graph, oxygen uptake rate is calculated for particular values of specific growth rate using the first order plus time delay model parameters 0.2, 0.3, 0.4, 0.5, 0.6 values of μ are also calculated in a similar manner as per the above procedure, since many information has to explain further, so remaining values are given in Table 3.

3.2. Development of PID controller adaptation algorithm

3.2.1. Estimation of process dynamic parameters

3.2.1.1. Gain coefficient algorithm inference

Based on model parameters estimation results presented in Table 3, the second order polynomial model is used to describe relationships between process gain and oxygen uptake rate at specific growth rate values in the interval 0.1-0.6 h^{-1}.

$$K=a_0+a_1(OUR)+a_2(OUR)^2 \quad (3.1)$$

The least square method is used for identification of the model parameter [38].

$$A = (F^T.F)^{-1}.F^T.(Y) \quad (3.2)$$

we put F data into the matrix it consists of x1 = free suitable 1, x2 = OUR(oxygen uptake rate) , x3= OUR^2(appendix Number 5).

$F = [x_1 \;\; x_2 \;\; x_3]$;

x1=[1 1 1 1 1 1];

x2=[4.6304 5.1194 5.6578 6.2529 7.6367 12.5927];

x3=[21.4406 26.2083 32.0107 39.0988 58.3192 158.5761];

The available data obtained matrix Y_o for the three parameters are K-gain coefficient, T- Time constant, τ- time delay respectively. The simplification gain coefficient K = f(OUR) is determined by the experimental function independence of oxygen uptake rate at point of the specific growth rate (0.1 - 0.6 h^{-1}) in matrix Y_x.

Y_o = [2.37 2.14 1.87 1.7 1.4 0.89];

The coefficients of least square model and study, to continue calculated, the model parameters a_0, a_1 and a_2 coefficient in the MATLAB simulation by using least square formula $A = (F^T.F)^{-1}.F^T.(Y)$. Therefore, the results are: a0= 4.8751, a1=-0.6863, a2=0.0294(appendix Number 6). After obtained model parameters of the gain coefficient from Equation 3.1, then the mathematical model process is obtained.

$K = 4.8751 - 0.6863.x_1+0.0294.x_2$

Estimating the functional independence of the oxygen uptake rate at specific values of specific growth rate in the MATLAB simulation software tool model Y_x:

Y_x = [2.3276 2.1322 1.9333 1.7332 1.3486 0.8949];

Now, the comparison between experimental and modelling results via graph:

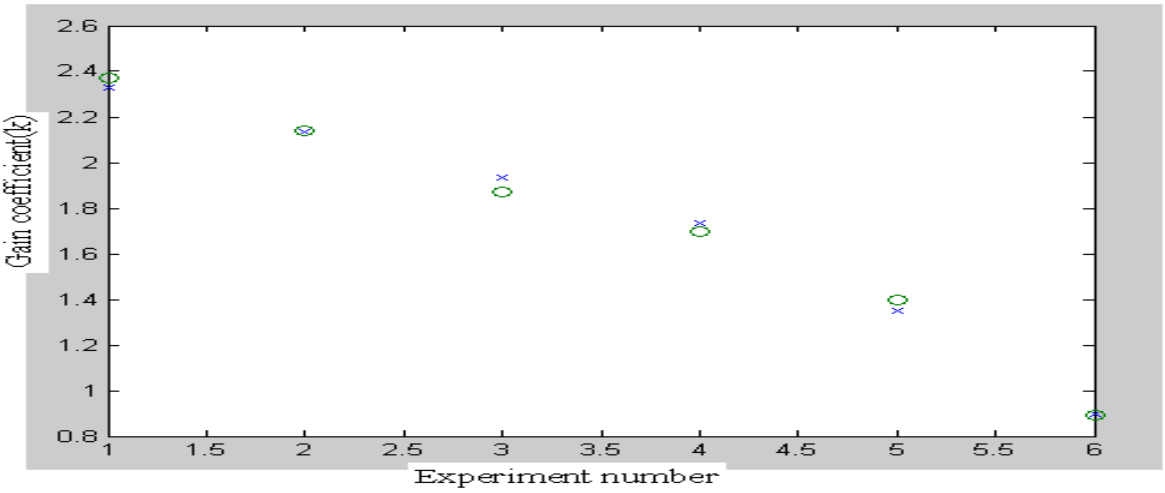

Figure 14. Graphical comparison of experimental and modelling results at 0.1 specific growth rate

As shown in the Figure 14, experimental results are determined by least square method, from a reaction curve dynamic parameters of gain(k), Time constant(T), Time delay(τ) are calculated that are substituted in the experimental results for different values of specific growth rate because to compare the results of reaction curve and experimental will approximately same as shown in the Figure 14, since reaction curve is identified 'o' and experimental results is identified 'x'. In this experiment simplification gain coefficient K = f(OUR) is determined by the experimental function independence of oxygen uptake rate at point of the specific growth rate ($0.1h^{-1}$) is Y_x = (2.3276, 2.1322, 1.9333, 1.7332, 1.3486, 0.8949) . As shown in the Figure 15, experimental results are determined by least square method, from a reaction curve dynamic parameters of gain(k), Time constant(T), Time delay(τ) are calculated that are substituted in the experimental results for different values of specific growth rate because to compare the results of reaction curve and experimental will approximately same as shown in the Figure 15, since reaction curve is identified 'o' and experimental results is identified 'x'. In this experiment simplification gain coefficient K = f(OUR) is determined by the experimental function independence of oxygen uptake rate at point of the specific growth rate ($0.2h^{-1}$) is y= (1.5735, 1.3435, 1.1057, 0.8794, 0.6209) .

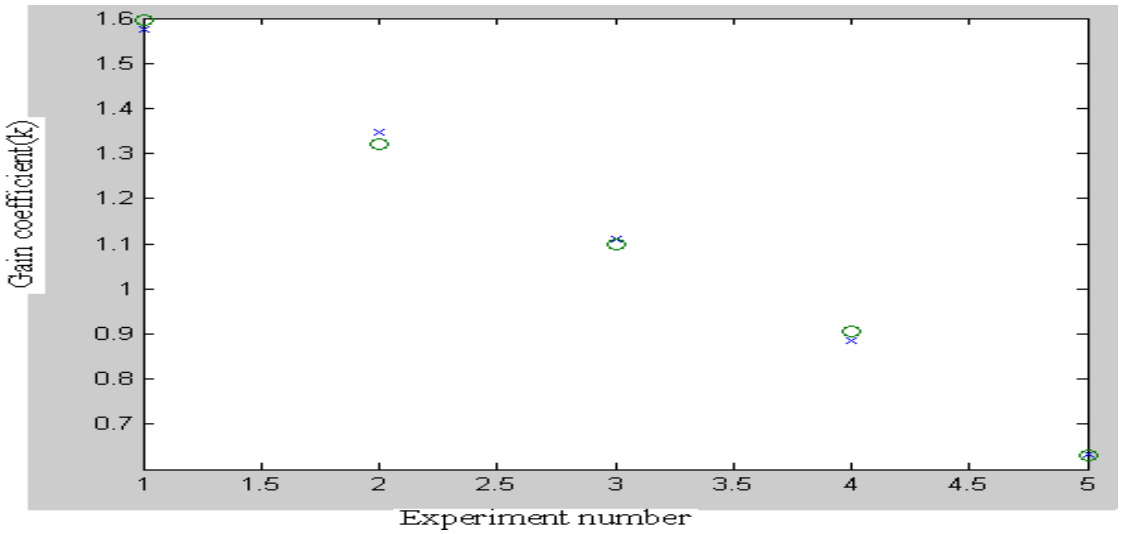

Figure 15. Graphical comparison of experimental and modelling results at 0.2 specific growth rate

As shown in the Figure 16, experimental results are determined by least square method, from a reaction curve dynamic parameters of gain(k), Time constant(T), Time delay(τ) are calculated that are substituted in the experimental results for different values of specific growth rate because to compare the results of reaction curve and experimental will approximately same as shown in the Figure 16, since reaction curve is identified 'o' and experimental results is identified 'x'.

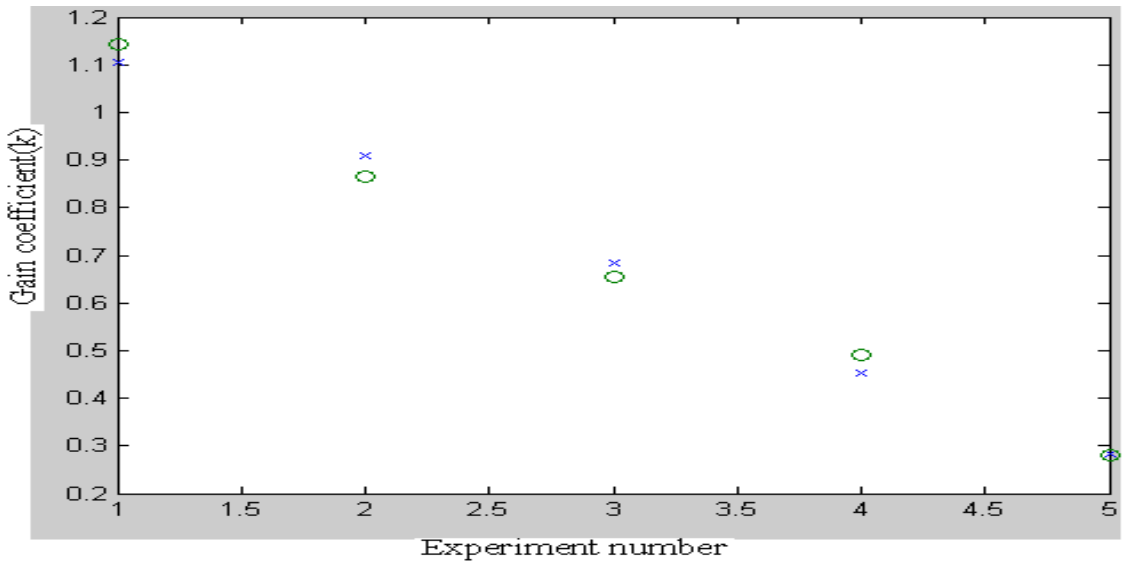

Figure 16. Graphical comparison of experimental and modelling results at 0.3 specific growth rate

In this experiment simplification gain coefficient K = f(OUR) is determined by the experimental function independence of oxygen uptake rate at point of the specific growth rate ($0.3h^{-1}$) is y= (1.1023, 0.9061, 0.6817, 0.4522, 0.2823). As shown in the Figure 17, experimental results are determined by least square method, from a reaction curve dynamic parameters of gain(k), Time constant(T), Time delay(τ) are calculated that are substituted in the experimental results for different values of specific growth rate because to compare the results of reaction curve and experimental will approximately same as shown in the Figure 17, since reaction curve is identified 'o' and experimental results is identified 'x'. In this experiment simplification gain coefficient K = f(OUR) is determined by the experimental function independence of oxygen uptake rate at point of the specific growth rate ($0.4h^{-1}$) is y= (0.8163, 0.5990, 0.3792, 0.2837). As shown in the Figure 18, experimental results are determined by least square method, from a reaction curve dynamic parameters of gain(k), Time constant(T), Time delay(τ) are calculated that are substituted in the experimental results for different values of specific growth rate because to compare the results of reaction curve and experimental will approximately as shown in the Figure 18, since reaction curve is identified 'o' and experimental results is identified 'x' .

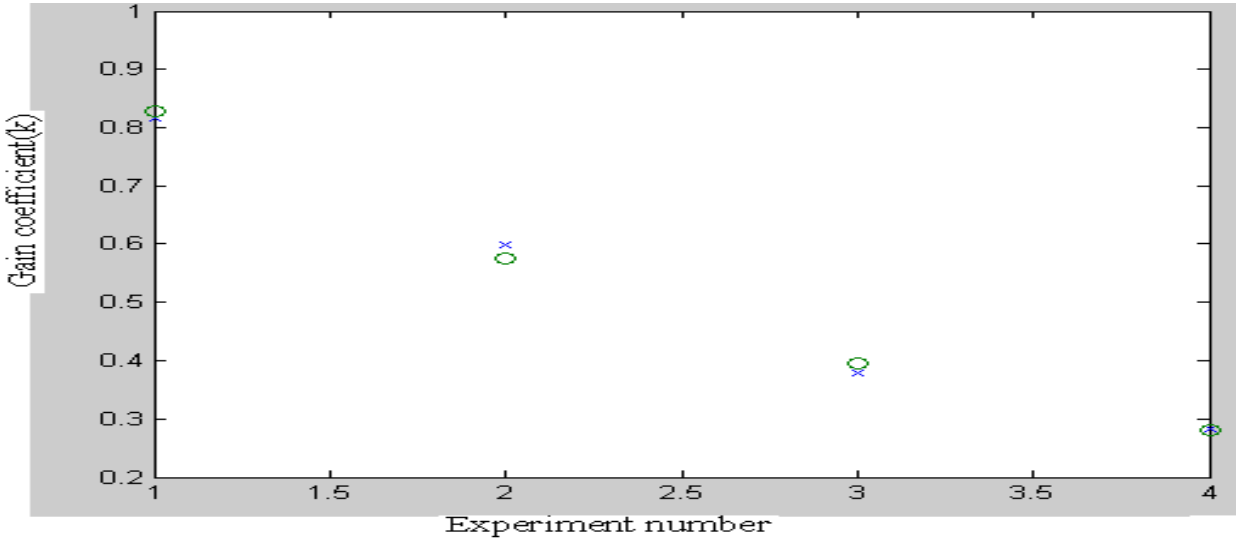

Figure 17. Graphical comparison of experimental and modelling results at 0.4 specific growth rate

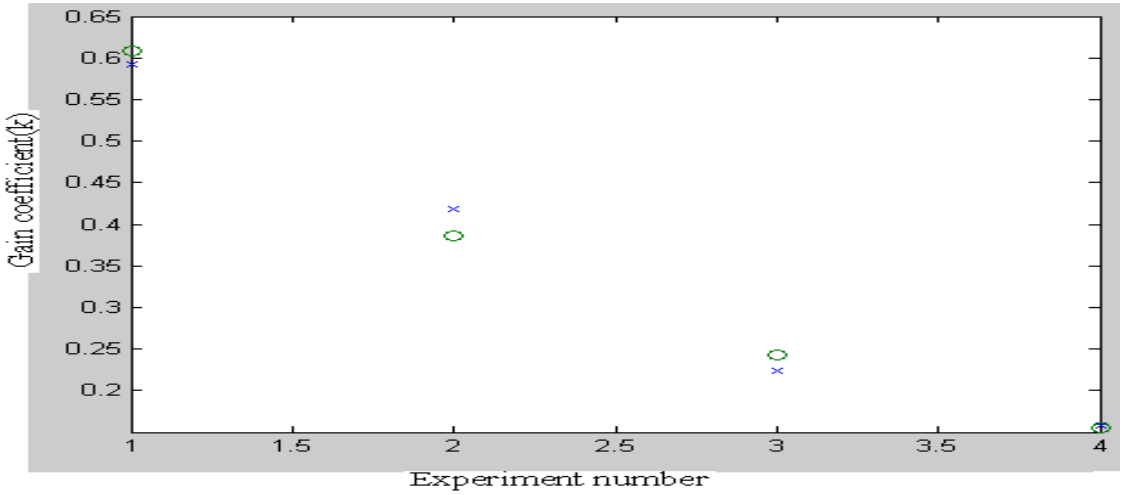

Figure 18. Graphical comparison of experimental and modelling results at 0.5 specific growth rate

In this experiment simplification gain coefficient K = f(OUR) is determined by the experimental function independence of oxygen uptake rate at point of the specific growth rate ($0.5h^{-1}$) is y= (0.5901, 0.4146, 0.2188, 0.1502).As shown in the Figure 19, experimental results are determined by least square method, from a reaction curve dynamic parameters of gain(k), Time constant(T), Time delay(τ) are calculated that are substituted in the experimental results for different values of specific growth rate because to compare the results of reaction curve and experimental will approximately same as shown in the Figure 19, since reaction curve is identified 'o' and experimental results is identified 'x'. In this experiment simplification gain coefficient K = f(OUR) is determined by the experimental function independence of oxygen uptake rate at the point of the specific growth rate ($0.6h^{-1}$) is y= (0.4050, 0.3145, 0.1496). The dynamic parameter dependence of the process depends on the oxygen uptake rate (OUR) and the dynamic parameters of the gain coefficient are determined by the specific set-point of specific growth rate, the modelled graphical representations of the reaction surface are shown in Figure 19. The reaction surface model program was presented in MATLAB/SIMULINK software.

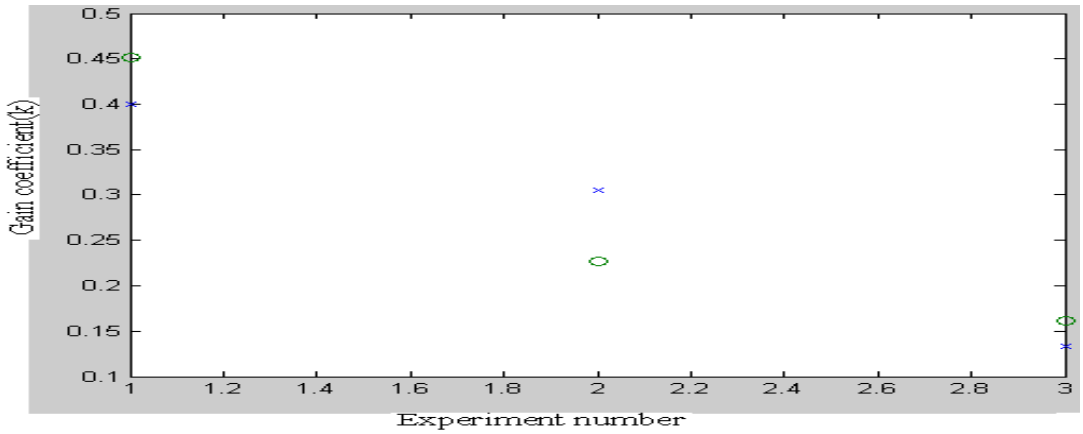

Figure 19. Graphical comparison of experimental and modelling results at 0.6 specific growth rate

The experiment results and modelling results are compared below as shown in Table 4, using the mathematical model equation, modelling parameters are obtained, which are compared in Table 4 and Table 3 shows the comparison of experimental and modelling study results.

Table 4. Comparison of the process gain experimental and model-based estimations at various SGR and OUR values

SL no	MU	OUR	K_{mod}	K_{LSM}
1	0.1	4.6304	2.37	2.3276
2	0.1	5.1194	2.14	2.1322
3	0.1	5.6578	1.87	1.9333
4	0.1	6.2529	1.7	1.73320
5	0.1	7.6367	1.4	1.3486
6	0.1	12.5927	0.89	0.8949
7	0.2	12.1234	1.595	1.5735
8	0.2	14.8081	1.32	1.3435
9	0.2	18.0872	1.1	1.1057
10	0.2	22.0922	0.905	0.8794
11	0.2	32.9967	0.63	0.6209
12	0.3	24.3869	1.1433	1.1023
13	0.3	32.9233	0.8666	0.9061
14	0.3	44.4447	0.65333	0.6817
15	0.3	59.9968	0.49	0.4522
16	0.3	109.0498	0.28	0.2823
17	0.4	43.2441	0.8275	0.8163
18	0.4	64.5238	0.575	0.5990
19	0.4	96.2653	0.395	0.3792
20	0.4	143.6018	0.28	0.2837
21	0.5	71.0925	0.608	0.5901
22	0.5	117.2368	0.386	0.4146
23	0.5	193.3035	0.243	0.2188
24	0.5	318.7199	0.155	0.1502
25	0.6	110.0697	0.451	0.4050
26	0.6	200.5792	0.2265	0.3145
27	0.6	365.4866	0.161	0.1496

3.2.1.2. Time constant algorithm inference

Based on model parameters estimation results presented in Table 3, the second order polynomial model is used to describe relationships between time constant and oxygen uptake rate at specific growth rate values in the interval 0.1-0.6 h^{-1}.

$$T = a_0+a_1(OUR)+a_2(OUR)^2 \quad (3.3)$$

The least square method is used for identification of the model parameter [38].

$$A = (F^T.F)^{-1}.F^T.(Y) \quad (3.4)$$

we put F data into the matrix it consists of x1 = free suitable 1, x2 = OUR(oxygen uptake rate) , x3= OUR^2(appendix Number 7).

$F = [x_1 \ x_2 \ x_3]$;

x1= [1 1 1 1 1 1];

x2= [4.6304 5.1194 5.6578 6.2529 7.6367 12.5927];

x3= [21.4406 26.2083 32.0107 39.0988 58.3192 158.5761];

The available data obtained matrix Y_o for the three parameters are K-gain coefficient, T- Time constant, τ- Time delay respectively. The simplification time constant T = f(OUR) is determined by the experimental functional independence of oxygen uptake rate at specific point of the specific growth rate (0.1 - 0.6 h^{-1}) in matrix Y_x.

Y_o = [0.0975 0.0869 0.0689 0.0627 0.0510 0.0408];

The coefficients of least square model and study, to continue calculated, the model parameters a_0, a_1 and a_2 coefficient in the MATLAB simulation by using least square formula $A = (F^T. F)^{-1}. F^T. (Y)$. Therefore, the results are a0= 0.2381, a1=-0.0400, a2=0.0020(appendix Number 8). After obtained model parameters of the time constant from Equation 3.3, then the mathematical model process is obtained.

$T = 0.2381-0.0400.x_1+0.0020.x_2$

Estimating the functional independence of oxygen uptake rate at specific values of specific growth rate in the MATLAB simulation software tool model Y_x, Now the comparison between experimental and modelling results via a graph.

Y_x = [0.0940 0.0838 0.0735 0.0633 0.0447 0.0404];

As shown in the Figure 20, experimental results are determined by least square method, from a reaction curve dynamic parameters of gain(k), Time constant(T), Time delay(τ) are calculated that are substituted in the experimental results for different values of specific growth rate because to compare the results of reaction curve and experimental will approximately same as shown in the Figure 20, since reaction curve is identified 'o' and experimental results is identified 'x'. In this experiment simplification time constant T = f(OUR) is determined by the experimental function independence of oxygen uptake rate at point of the specific growth rate ($0.1h^{-1}$) is Y_x = (0.0940, 0.0838, 0.0735, 0.0633, 0.0447, 0.0404).

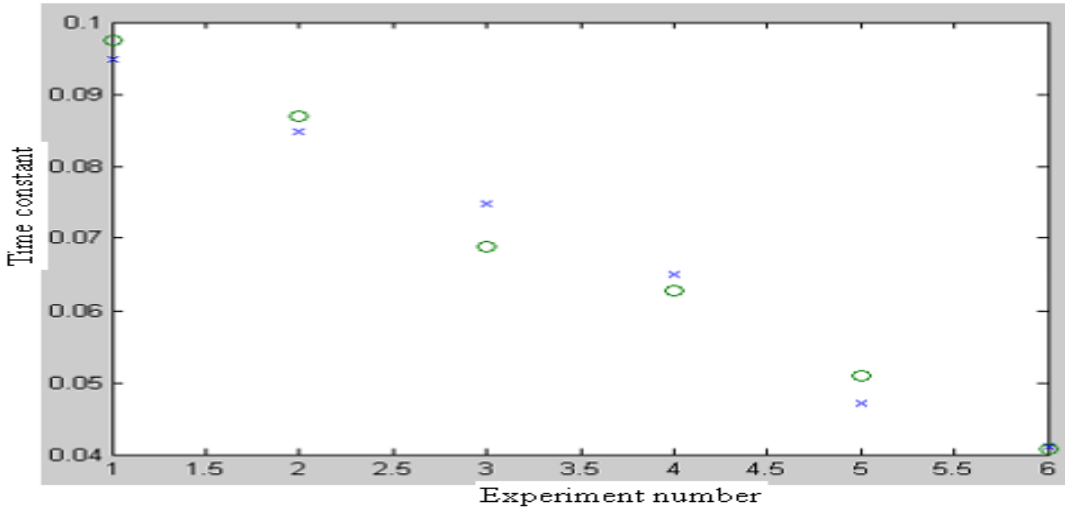

Figure 20. Graphical comparison of experimental and modelling results at 0.1 specific growth rate

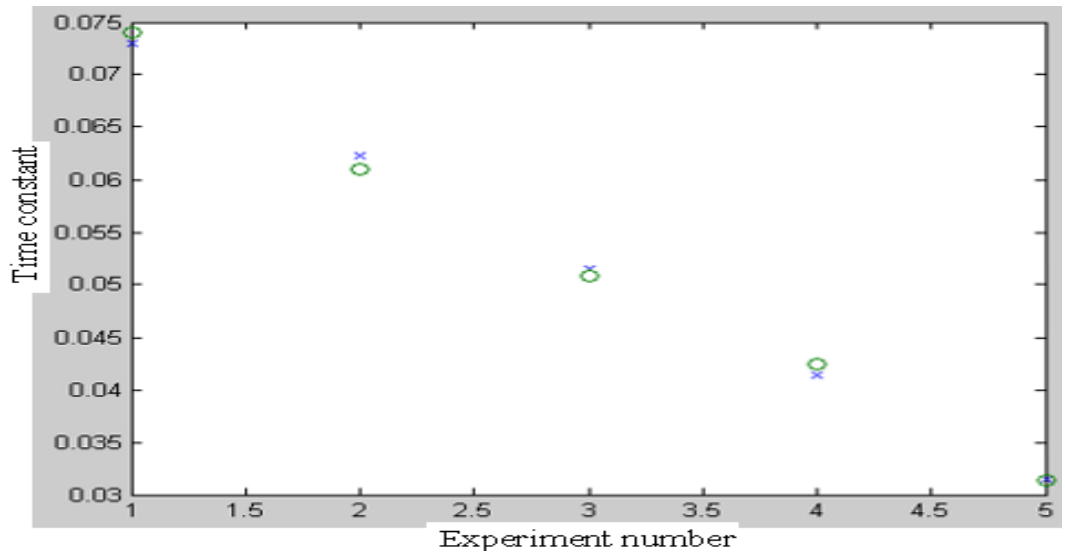

Figure 21. Graphical comparison of experimental and modelling results at 0.2 specific growth rate

As shown in the Figure 21, experimental results are determined by least square method, from a reaction curve dynamic parameters of gain(k), Time constant(T), Time delay(τ) are calculated that are substituted in the experimental results for different values of specific growth rate because to compare the results of reaction curve and experimental will approximately same as shown in the Figure 21, since reaction curve is identified 'o' and experimental results is identified 'x'. In this experiment simplification time constant T = f(OUR) is determined by the experimental function independence of oxygen uptake rate at point of the specific growth rate ($0.2h^{-1}$) is Y_x = (0.0726, 0.0619, 0.0509, 0.0407, 0.0305). As shown in the Figure 22, experimental results are determined by least square method, from a reaction curve dynamic parameters of gain(k), Time constant(T), Time delay(τ) are calculated that are substituted in the experimental results for different values of specific growth rate because to compare the results of reaction curve and experimental will approximately same as shown in the Figure 22, since reaction curve is identified 'o' and experimental results is identified 'x'. In this experiment simplification time constant T = f(OUR) is determined by the experimental function independence of oxygen uptake rate at point of the specific growth rate ($0.3h^{-1}$) is Y_x = (0.0661, 0.0550, 0.0425, 0.0300, 0.0238).

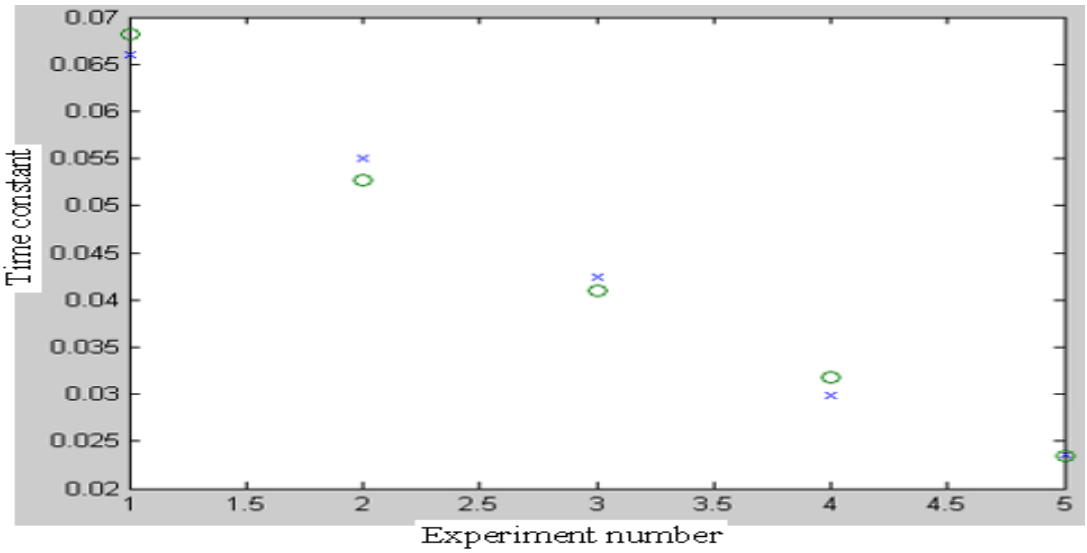

Figure 22. Graphical comparison of experimental and modelling results at 0.3 specific growth rate

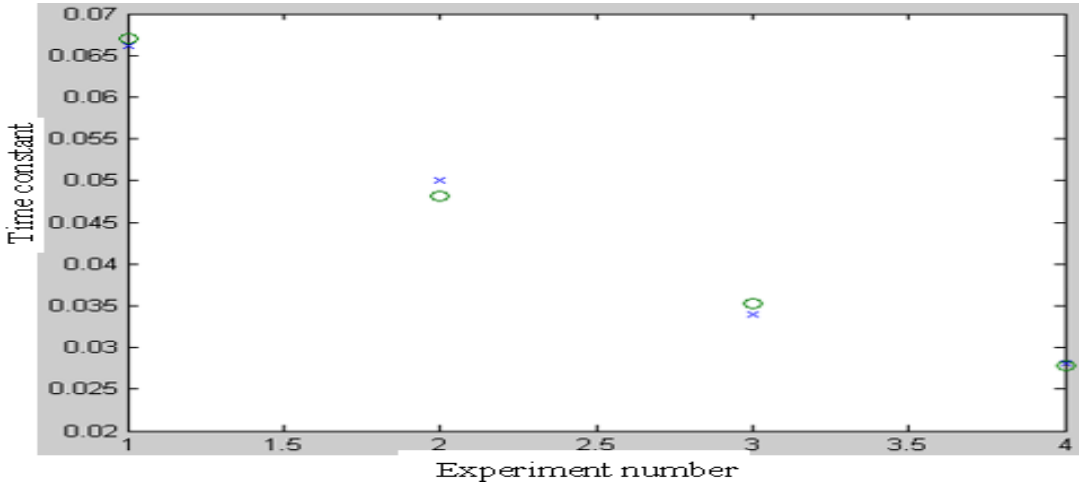

Figure 23. Graphical comparison of experimental and modelling results at 0.4 specific growth rate

As shown in the Figure 23, experimental results are determined by least square method, from a reaction curve dynamic parameters of gain(k), Time constant(T), Time delay(τ) are calculated that are substituted in the experimental results for different values of specific growth rate because to compare the results of reaction curve and experimental will approximately same as shown in the Figure 23, since reaction curve is identified 'o' and experimental results is identified 'x'. In this experiment simplification time constant T = f(OUR) is determined by the experimental function independence of oxygen uptake rate at point of the specific growth rate ($0.4h^{-1}$) is Y_x = (0.0652, 0.0485, 0.0317, 0.0274). As shown in the Figure 24, experimental results are determined by least square method, from a reaction curve dynamic parameters of gain(k), Time constant(T), Time delay(τ) are calculated that are substituted in the experimental results for different values of specific growth rate because to compare the results of reaction curve and experimental will approximately same as shown in the Figure 24, since reaction curve is identified 'o' and experimental results is identified 'x'. In this experiment simplification time constant T = f(OUR) is determined by the experimental function independence of oxygen uptake rate at point of the specific growth rate ($0.5h^{-1}$) is Y_x = (0.0686, 0.0513, 0.0324, 0.0271).

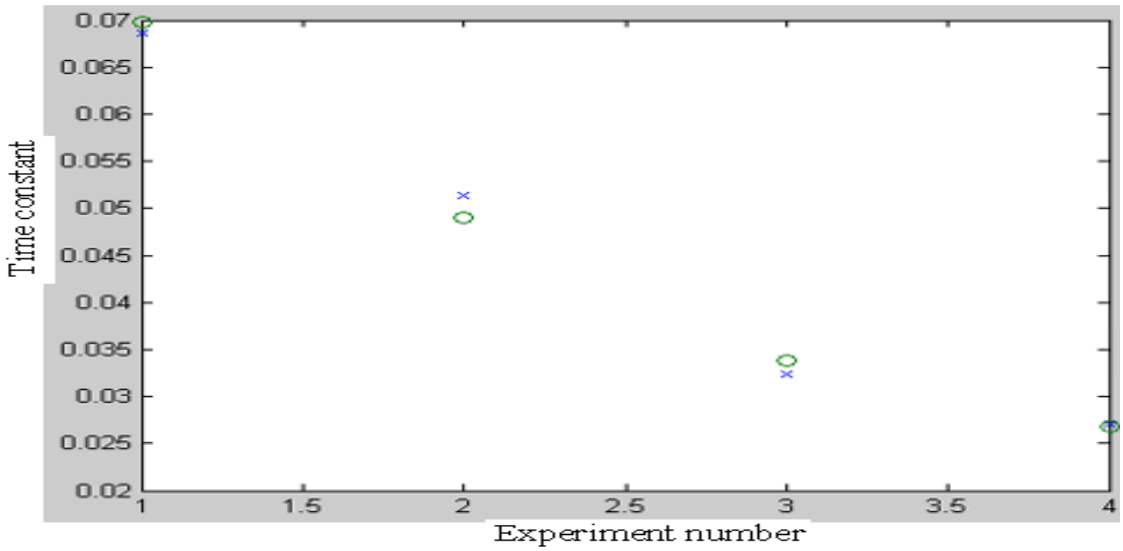

Figure 24. Graphical comparison of experimental and modelling results at 0.5 specific growth rate

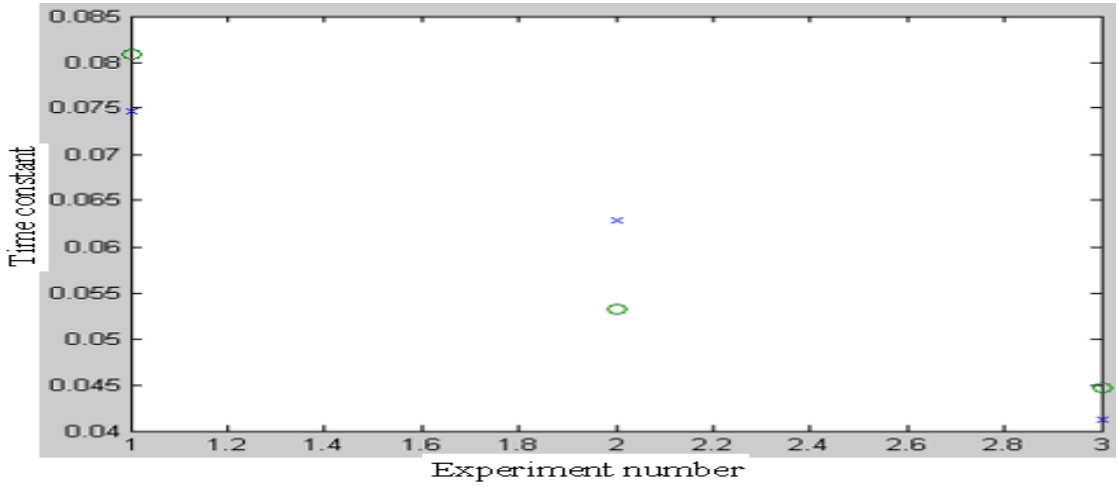

Figure 25. Graphical comparison of experimental and modelling results at 0.6 specific growth rate

As shown in the Figure 25, experimental results are determined by least square method, from a reaction curve dynamic parameters of gain(k), Time constant(T), Time delay(τ) are calculated that are substituted in the experimental results for different values of specific growth rate because to compare the results of reaction curve and experimental will approximately same as shown in the Figure 25, since reaction curve is identified 'o' and experimental results is identified 'x'. In this experiment simplification time constant T = f(OUR) is determined by the experimental function independence of oxygen uptake rate at point of the specific growth rate ($0.6h^{-1}$) is Y_x = (0.0746, 0.0628, 0.0413). The dynamic parameter dependence of the process depends on the oxygen uptake rate (OUR) and the dynamic parameters of the time constant are determined by the specific set-point of specific growth rate, the modelled graphical representations of the reaction surface are shown in Figure 25. The Reaction Surface Model program was presented in MATLAB/SIMULINK software. The experiment results and modelling results are compared in the below Table 5, using the obtained mathematical model equation, modelling parameters are found, which are compared in Table 5 and Table 3 shows the comparison of experimental and modelling study results.

Table 5. Comparison of the time constant experimental and model-based estimations at various SGR and OUR values

SL no	MU	OUR	T_{mod}	T_{LSM}
1	0.1	4.6304	0.0975	0.0940
2	0.1	5.1194	0.0869	0.0838
3	0.1	5.6578	0.0689	0.0735
4	0.1	6.2529	0.0627	0.0633
5	0.1	7.6367	0.0510	0.0447
6	0.1	12.5927	0.0408	0.0404
7	0.2	12.1234	0.07395	0.0726
8	0.2	14.8081	0.06105	0.0619
9	0.2	18.0872	0.05085	0.0509
10	0.2	22.0922	0.0425	0.0407
11	0.2	32.9967	0.03125	0.0305
12	0.3	24.3869	0.0681	0.0661
13	0.3	32.9233	0.05265	0.0550
14	0.3	44.4447	0.04095	0.0425
15	0.3	59.9968	0.0318	0.0300

16	0.3	109.0498	0.0234	0.0238
17	0.4	43.2441	0.06705	0.0652
18	0.4	64.5238	0.04815	0.0485
19	0.4	96.2653	0.03525	0.0317
20	0.4	143.6018	0.0278	0.0274
21	0.5	71.0925	0.06975	0.0686
22	0.5	117.2368	0.04905	0.0513
23	0.5	193.3035	0.03375	0.0324
24	0.5	318.7199	0.02685	0.0271
25	0.6	110.0697	0.08085	0.0746
26	0.6	200.5792	0.05325	0.0628
27	0.6	365.4866	0.0447	0.0413

3.2.1.3. Time delay algorithm inference

Based on model parameters estimation results presented in Table 3, the second order polynomial model is used to describe relationships between time delay and oxygen uptake rate at specific growth rate values in the interval 0.1-0.6 h^{-1}.

$$\tau = a_0+a_1(OUR)+a_2(OUR)^2 \quad (3.5)$$

The least square method is used for identification of the model parameter [38].

$$A = (F^T. F)^{-1}. F^T. (Y) \quad (3.6)$$

we put F data into the matrix it consists of x1 = free suitable 1, x2 = OUR(oxygen uptake rate) , x3= OUR^2(appendix Number 9).

F = [x_1 x_2 x_3]; x1= [1 1 1 1 1 1]; x2= [4.6304 5.1194 5.6578 6.2529 7.6367 12.5927];

x3=[21.4406 26.2083 32.0107 39.0988 58.3192 158.5761];

The available data obtained matrix Y_o for the three parameters are K-gain coefficient, T- Time constant, τ- Time delay respectively. The simplification time delay τ = f(OUR) is determined by the experimental functional independence of oxygen uptake rate at specific point of the specific growth rate (0.1 - 0.6 h^{-1}) in matrix Y_x.

Y_o = [0.0099 0.0095 0.0087 0.0077 0.0066 0.0056];

The coefficients of least square model and study, to continue calculated, the model parameters a_0, a_1 and a_2 coefficient in the MATLAB simulation by using least square formula $A = (F^T. F)^{-1}. F^T. (Y)$. Therefore, the results are a0= 0.01961, a1=-0.0026, a2=1.2052e^{-04}(appendix Number 10). After obtained model parameters of the time delay from Equation 3.5, then the mathematical model process is obtained.

$\tau = 0.2381-0.0400.x_1+0.0020.x_2$

Estimating the functional independence of oxygen uptake rate at specific values of specific growth rate in the MATLAB simulation software tool model Y_x, Now the comparison between experimental and modelling results via graph:

Y_x = [0.0102 0.0095 0.0088 0.0081 0.0068 0.0056];

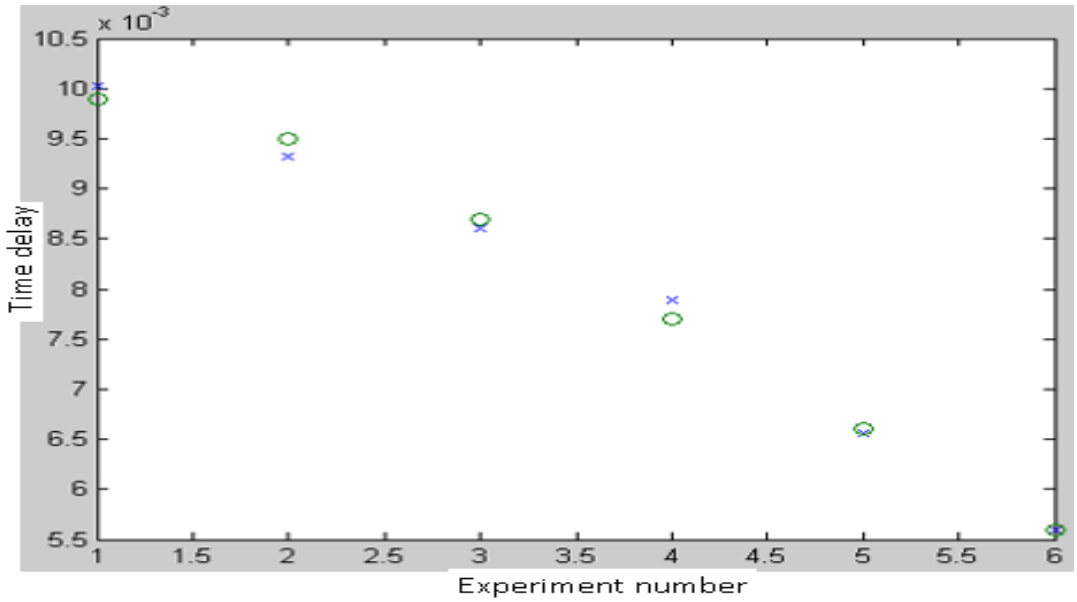

Figure 26. Graphical comparison of experimental and modelling results at 0.1 specific growth rate

As shown in the Figure 26, experimental results are determined by least square method, from a reaction curve dynamic parameters of gain(k), Time constant(T), Time delay(τ) are calculated that are substituted in the experimental results for different values of specific growth rate because to compare the results of reaction curve and experimental will approximately same as shown in the Figure 26, since reaction curve is identified 'o' and experimental results is identified 'x'. In this experiment simplification time delay τ = f(OUR) is determined by the experimental function independence of oxygen uptake rate at point of the specific growth rate ($0.1h^{-1}$) is Y_x = (0.0102, 0.0095, 0.0088, 0.0081, 0.0068, 0.0056). As shown in the Figure 27, experimental results are determined by least square method, from a reaction curve dynamic parameters of gain(k), Time constant(T), Time delay(τ) are calculated that are substituted in the experimental results for different values of specific growth rate because to compare the results of reaction curve and experimental will approximately same as shown in the Figure 27, since reaction curve is identified 'o' and experimental results is identified 'x'. In this experiment simplification time delay τ = f(OUR) is determined by the experimental function independence of oxygen uptake rate at point of the specific growth rate ($0.2h^{-1}$) is Y_x = (0.0119, 0.0116, 0.0112, 0.0108, 0.0099).

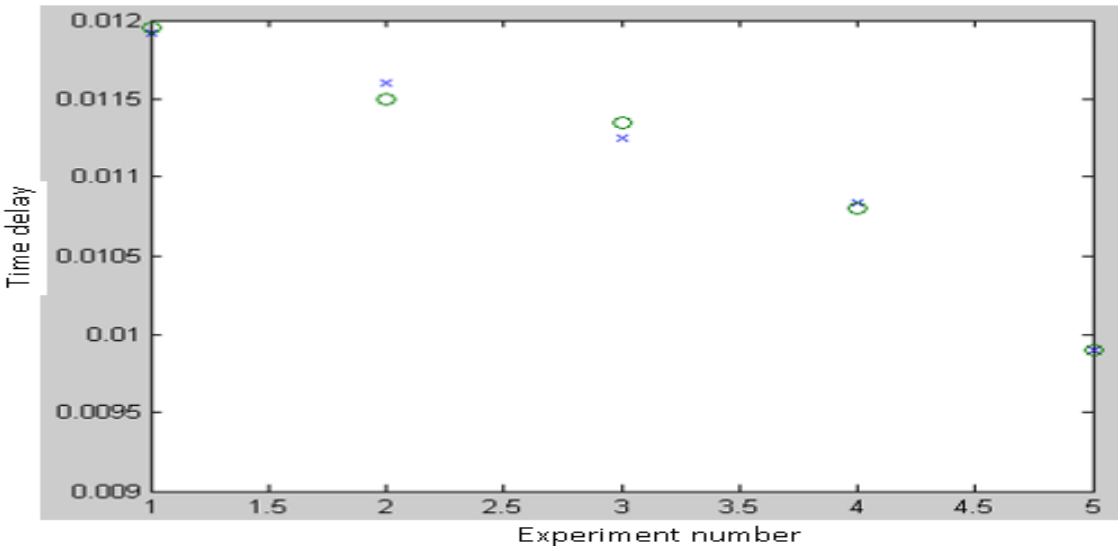

Figure 27. Graphical comparison of experimental and modelling results at 0.2 specific growth rate

As shown in the Figure 28, experimental results are determined by least square method, from a reaction curve dynamic parameters of gain(k), Time constant(T), Time delay(τ) are calculated that are substituted in the experimental results for different values of specific growth rate because to compare the results of reaction curve and experimental will approximately same as shown in the Figure 28, since reaction curve is identified 'o' and experimental results is identified 'x'.

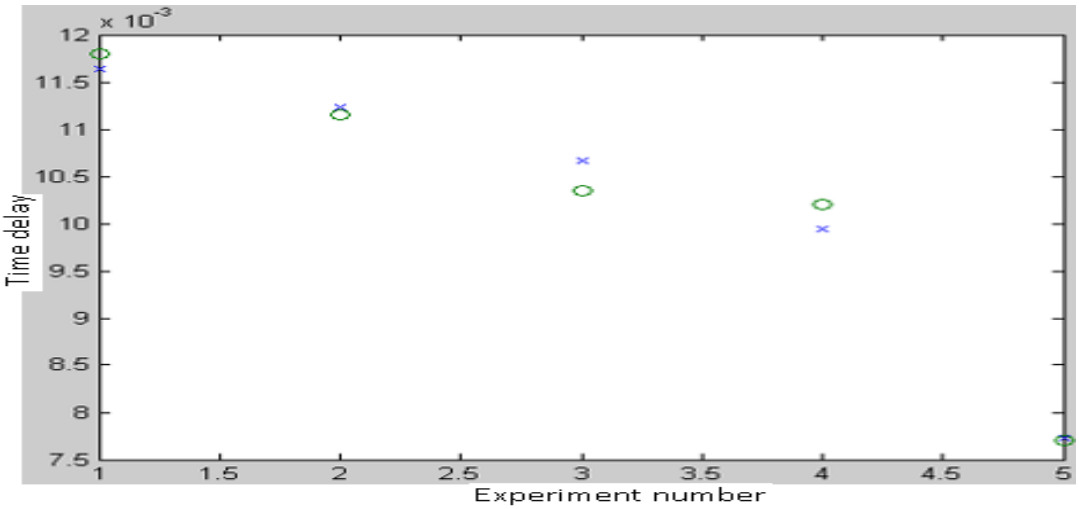

Figure 28. Graphical comparison of experimental and modelling results at 0.3 specific growth rate

In this experiment simplification time delay τ = f(OUR) is determined by the experimental function independence of oxygen uptake rate at point of the specific growth rate ($0.3h^{-1}$) is Y_x = (0.0117, 0.0113, 0.0107, 0.0100, 0.0078). As shown in the Figure 29, experimental results are determined by least square method, from a reaction curve dynamic parameters of gain(k), Time constant(T), Time delay(τ) are calculated that are substituted in the experimental results for different values of specific growth rate because to compare the results of reaction curve and experimental will approximately same as shown in the Figure 29 , since reaction curve is identified 'o' and experimental results is identified 'x'.

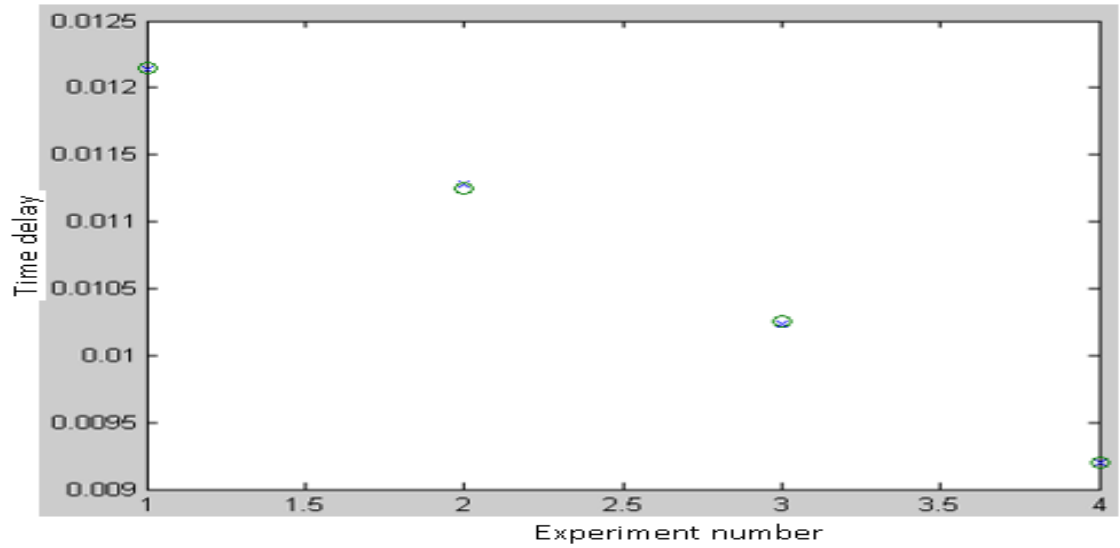

Figure 29. Graphical comparison of experimental and modelling results at 0.4 specific growth rate

In this experiment simplification time delay τ = f(OUR) is determined by the experimental function independence of oxygen uptake rate at point of the specific growth rate ($0.4h^{-1}$) is Y_x = (0.0122, 0.0113, 0.0103, 0.0092).

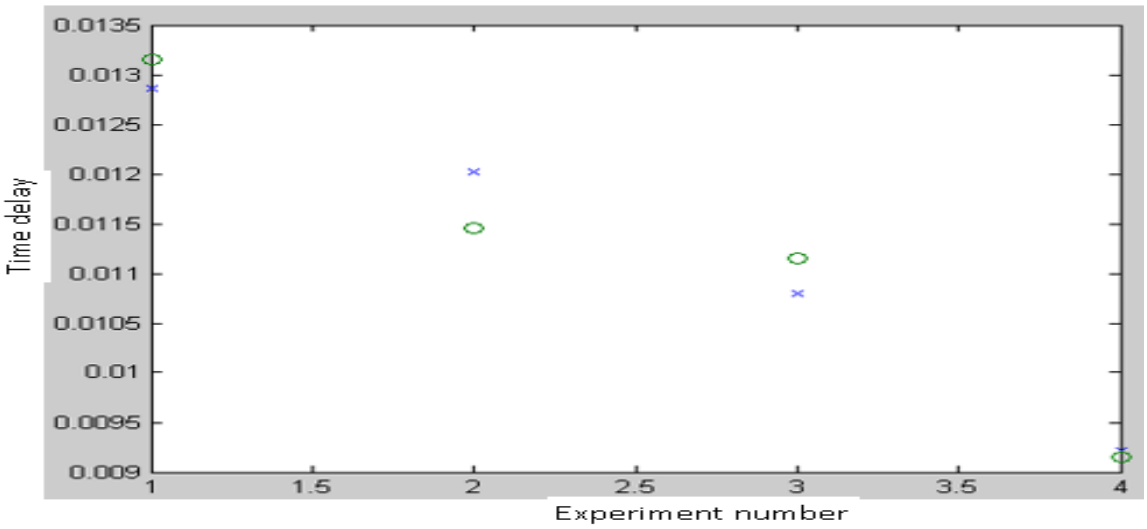

Figure 30. Graphical comparison of experimental and modelling results at 0.5 specific growth rate

As shown in the Figure 30, experimental results are determined by least square method, from a reaction curve dynamic parameters of gain(k), Time constant(T), Time delay(τ) are calculated that are substituted in the experimental results for different values of specific growth rate because to compare the results of reaction curve and experimental will approximately same as shown in the Figure 30, since reaction curve is identified 'o' and experimental results is identified 'x'. In this experiment simplification time delay τ = f(OUR) is determined by the experimental function independence of oxygen uptake rate at point of the specific growth rate ($0.5h^{-1}$) is Y_x = (0.0129, 0.0120, 0.0108, 0.0092).

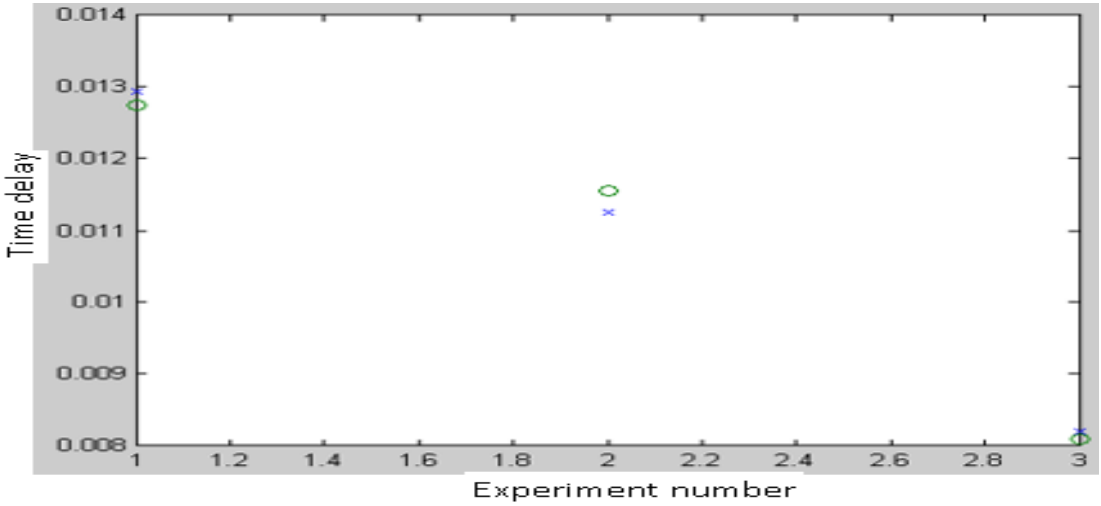

Figure 31. Graphical comparison of experimental and modelling results at 0.6 specific growth rate

As shown in the Figure 31, experimental results are determined by least square method, from a reaction curve dynamic parameters of gain(k), Time constant(T), Time delay(τ) are calculated that are substituted in the experimental results for different values of specific growth rate because to compare the results of reaction curve and experimental will approximately same as shown in the Figure 31, since reaction curve is identified 'o' and experimental results is identified 'x'. In this experiment simplification time delay τ = f(OUR) is determined by the experimental function independence of oxygen uptake rate at point of the specific growth rate ($0.6h^{-1}$) is Y_x = (0.0130, 0.0113, 0.0082).

The dynamic parameter dependence of the process depends on the oxygen uptake rate(OUR) and the dynamic parameters of the time delay are determined by the specific set-point of specific growth rate, the modelled graphical representations of the reaction surface are shown in Figure 31. The Reaction Surface Model program was presented in MATLAB/SIMULINK software. The experiment and modelling results are compared as shown in Table 6, using the obtained mathematical model equation, modelling parameters are obtained, which are compared in Table 6 and Table 3 shows the comparison of experimental and modelling study results.

Table 6. Comparison of the time delay experimental and model-based estimations at various SGR and OUR values

SL no	MU	OUR	τ_{mod}	τ_{LSM}
1	0.1	4.6304	0.0099	0.0102
2	0.1	5.1194	0.0095	0.0095
3	0.1	5.6578	0.0087	0.0088
4	0.1	6.2529	0.0077	0.0081
5	0.1	7.6367	0.0066	0.0068
6	0.1	12.5927	0.0056	0.0056
7	0.2	12.1234	0.01195	0.0119
8	0.2	14.8081	0.0115	0.0116
9	0.2	18.0872	0.01135	0.0112
10	0.2	22.0922	0.0108	0.0108
11	0.2	32.9967	0.0099	0.0099
12	0.3	24.3869	0.0118	0.0117
13	0.3	32.9233	0.01115	0.0113
14	0.3	44.4447	0.01035	0.0107

15	0.3	59.9968	0.0102	0.0100
16	0.3	109.0498	0.0077	0.0078
17	0.4	43.2441	0.01215	0.0122
18	0.4	64.5238	0.01125	0.0113
19	0.4	96.2653	0.01025	0.0103
20	0.4	143.6018	0.0092	0.0092
21	0.5	71.0925	0.01315	0.0129
22	0.5	117.2368	0.01145	0.0120
23	0.5	193.3035	0.01115	0.0108
24	0.5	318.7199	0.00915	0.0092
25	0.6	110.0697	0.01275	0.0130
26	0.6	200.5792	0.01155	0.0113
27	0.6	365.4866	0.0081	0.0082

3.2.2. Development of controller gain scheduling algorithm

a) Design of ACS:

The model of the control system, which compensates for the effect of the two major parts to develop the adaptive system, shown in Figure 32. The model system consists of(appendix Number 11, Number 12, Number 14, Number 15 and Number 16):

- Controller adaptation subsystem
- PID controller subsystem
- DEE block (Differential Equation Editor)
- Process dynamic parameter subsystem
- Measurement noise modelling subsystem

Table 7. process model input

Variable	Description	Inputs
U	Feeding rate	U (1)

Table 8. process model outputs

Variable	Description	Output
x	Biomass concentration	X (1)
s	Substrate concentration	X (2)
μ(SGR)	Specific growth rate	X (3)
v	Volume broth	X (4)
OUR	Oxygen uptake rate	OUR

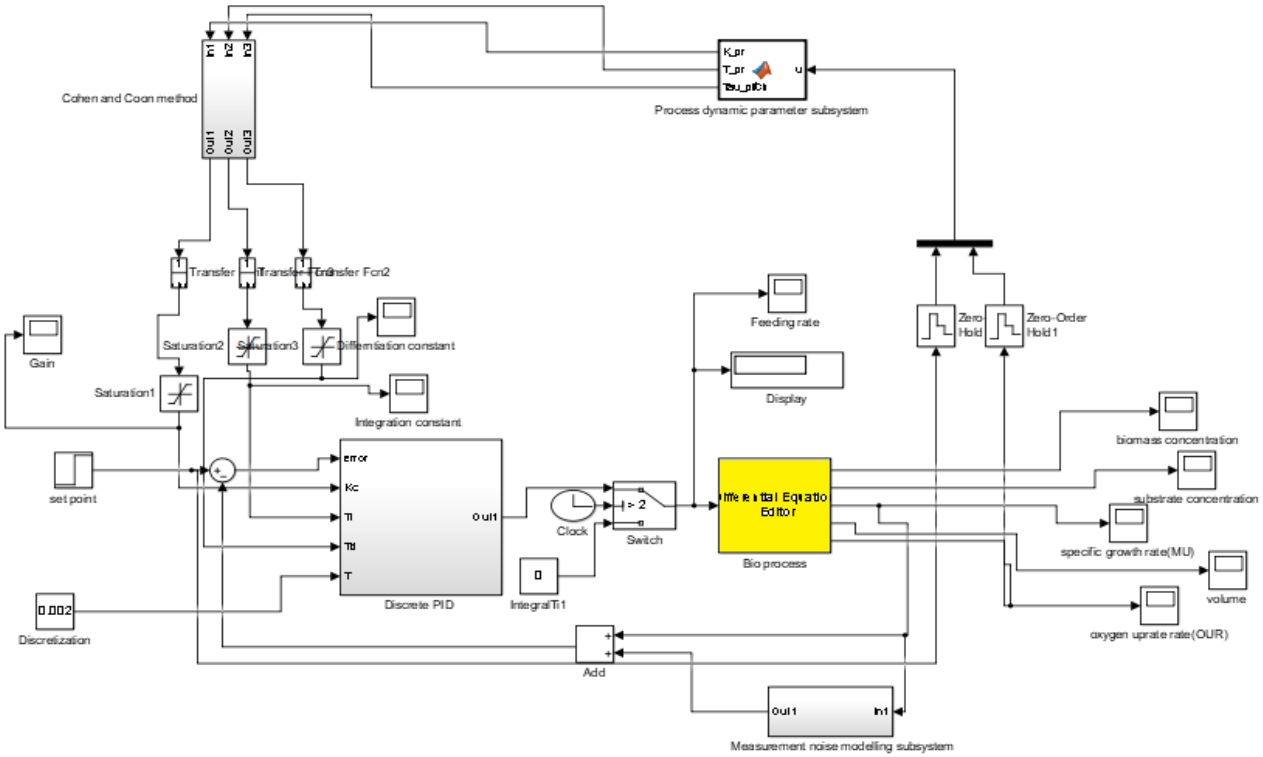

Figure 32. Block scheme of adaptative control system realized in MATLAB /SIMULINK environment

b) On-line estimation of control process dynamic parameters

The set algorithm parameter consists of the second order polynomial rules that calculate the gain coefficient(K), time constant(T) and time delay(τ) respectively. After the model is built in MATLAB/SIMULINK tool, the second order of the polynomial rules is entered the subsystem block containing the one variable, oxygen uptake rate at specific values of the specific growth rate [38]. The gain coefficient is calculated by function(appendix Number 11):

$$K=a_0+a_1(OUR)+a_2(OUR)^2 \quad (3.7)$$

The time constant is calculated by function:

$$T=a_0+a_1(OUR)+a_2(OUR)^2 \quad (3.8)$$

The time delay is calculated by function:

$$\tau=a_0+a_1(OUR)+a_2(OUR)^2 \quad (3.9)$$

Note: I have analyzed the data and found the reason for the 2 variable model identification problem. The problem is that the ranges of the OUR variation at various levels of mu are very different and the data obtained is not suitable for identification of the 2 variable relationships, covering full observed ranges of the mu and the OUR variations. So, for the μ controller adaptation, the algorithm based on the expert "IF-THEN" rules and the single variable OUR relationships can be used.

c) PID controller gain scheduling algorithm

The tuning method was selected to tune discrete PID control is calculated by using Cohen and Coon tuning rules [39]. They consist of a regulator gain factor, calculated according to the formula in the

book, the integration time constant, calculated according to the formula in the book and the differentiation time constant, calculated according to the formula in the book. The formulas assume that the process is characterized by the first series of suffixes. the duration of the charge and the range of the constant ratio of time are in the rules of adjustment(appendix Number 12):

$$0.1<\tau_{pr}/T_{pr}<1.0 \tag{3.10}$$

A model MATLAB / SIMULINK developed for the tuning parameter compensation, calculated using subsystems block. Tuning parameters the regulator gain coefficient is calculated according to the formula [39]:

$$K_r(t_k) = \frac{T_{pr}(t_k)}{K_{pr}\,(t_k)\tau_{pr}(t_k)}\left(1.33 + \frac{\tau_{pr}(t_k)}{4T_{pr}(t_k)}\right) \tag{3.11}$$

Integration time constant is calculated according to the formula [39]:

$$T_i(t_k) = \frac{32+6\frac{\tau_{pr}(t_k)}{T_{pr}(t_k)}}{13+8\frac{\tau_{pr}(t_k)}{T_{pr}(t_k)}}\tau_{pr}(t_k) \tag{3.12}$$

The differentiation time constant is calculated according to the formula [39]:

$$T_d(t_k) = \frac{4}{11+2\frac{\tau_{pr}(t_k)}{T_{pr}(t_k)}}\tau_{pr}(t_k) \tag{3.13}$$

d) The control algorithm of discrete PID controller:

The control system PID controller model consists of the input parameters that are entered in the formula (3.15). The obtained by rotating the engine of the modelled air water cooler according to the given data parameters available(appendix Number 15).

- Present error signal - e_n
- Previous error signal - e_{n-1}
- Last two previous error signal - e_{n-2}
- Proportional gain - K_r
- Integration time constant - T_i
- Differentiation time constant - T_d
- Discretization step – T

Frequently used algorithms used by the regulator are reflected in the change of the controlling effect [39]:

$$U_n = U_{n-1} + \Delta U_n \tag{3.14}$$

All data is entered in a formula prepared by the PID editor, which calculates the engine brush N. The discrete change in the control effect of the PID controller is calculated according to the formula [39]:

$$\Delta U_n = \mathrm{k_r}[\left(1 + \frac{\mathrm{T_d}}{\mathrm{T}} + \frac{\mathrm{T}}{\mathrm{T_i}}\right)e_n - \left(1 + \frac{2\mathrm{T_d}}{\mathrm{T}}\right)e_{n-1} + \frac{\mathrm{T_d}}{\mathrm{T}}e_{n-2} \tag{3.15}$$

4. SIMULATION RESULTS OF ORDINARY AND ADAPTIVE CONTROL SYSTEMS PERFORMANCE AND DISCUSSION OF RESULTS

Experiment 1: The set-point of specific growth rate(μ) was changed from μ_{set} = 0.0501 h^{-1} to μ_{set} = 0.3 h^{-1} and simulation time 6 (h) as shown in Figure 33. The overshoot and settling time of the adaptive system is decreased 42 %, 34% compared to non-adaptive system respectively.

Table 9. PID controller tuning parameters

Model parameters (Initial 0.0501; Final 0.3)	Adaptive system	Non-adaptive system
Gain proportional (Kc)	6.854	10
Integration time constant (Ti)	0.02669	0.0347
Differentiation time constant (Td)	0.004103	0.00524

Experiment 2: The set-point of specific growth rate(μ) was changed from μ_{set} = 0.5 h^{-1} to μ_{set} = 0.6 h^{-1} and simulation time 8 (h) as shown in Figure 34. The overshoot and settling time of an adaptive system is increased 73% and decreased 25% compared to non-adaptive system.

Table 10. PID controller model parameters

Model parameters (Initial 0.5; Final 0.6)	Adaptive system	Non-adaptive system
Gain proportional (Kc)	34.75	10
Integration time constant (Ti)	0.0219	0.0313
Differentiation time constant (Td)	0.0034	0.0048

Experiment 3: The set-point of specific growth rate(μ) was changed from μ_{set} = 0.2 h^{-1} to μ_{set} = 0.6 h^{-1} and simulation time 8 (h) as shown in Figure 35. The overshoot and settling time of the adaptive system is decreased 11 %, decreased 50% compared to non-adaptive system respectively.

Table 11. PID controller model parameters

Model parameters (Initial 0.2; Final 0.6)	Adaptive system	Non-adaptive system
Gain proportional (Kc)	17.05	30.5
Integration time constant (Ti)	0.02946	0.0288
Differentiation time constant (Td)	0.0045	0.0044

Experiment 4:The set-point of specific growth rate(μ) was changed from μ_{set} = 0.4 h^{-1} to μ_{set} = 0.5 $h^{-1}$and simulation time 6 (h) as shown in the Figure 36. The overshoot and settling time of the adaptive system is decreased 19%, decreased 67% compared to non-adaptive system respectively.

Table 12. PID controller model parameters

Model parameters (Initial 0.4; Final 0.5)	Adaptive system	Non-adaptive system
Gain proportional (Kc)	21.75	20
Integration time constant (Ti)	0.022	0.027
Differentiation time constant (Td)	0.0035	0.0041

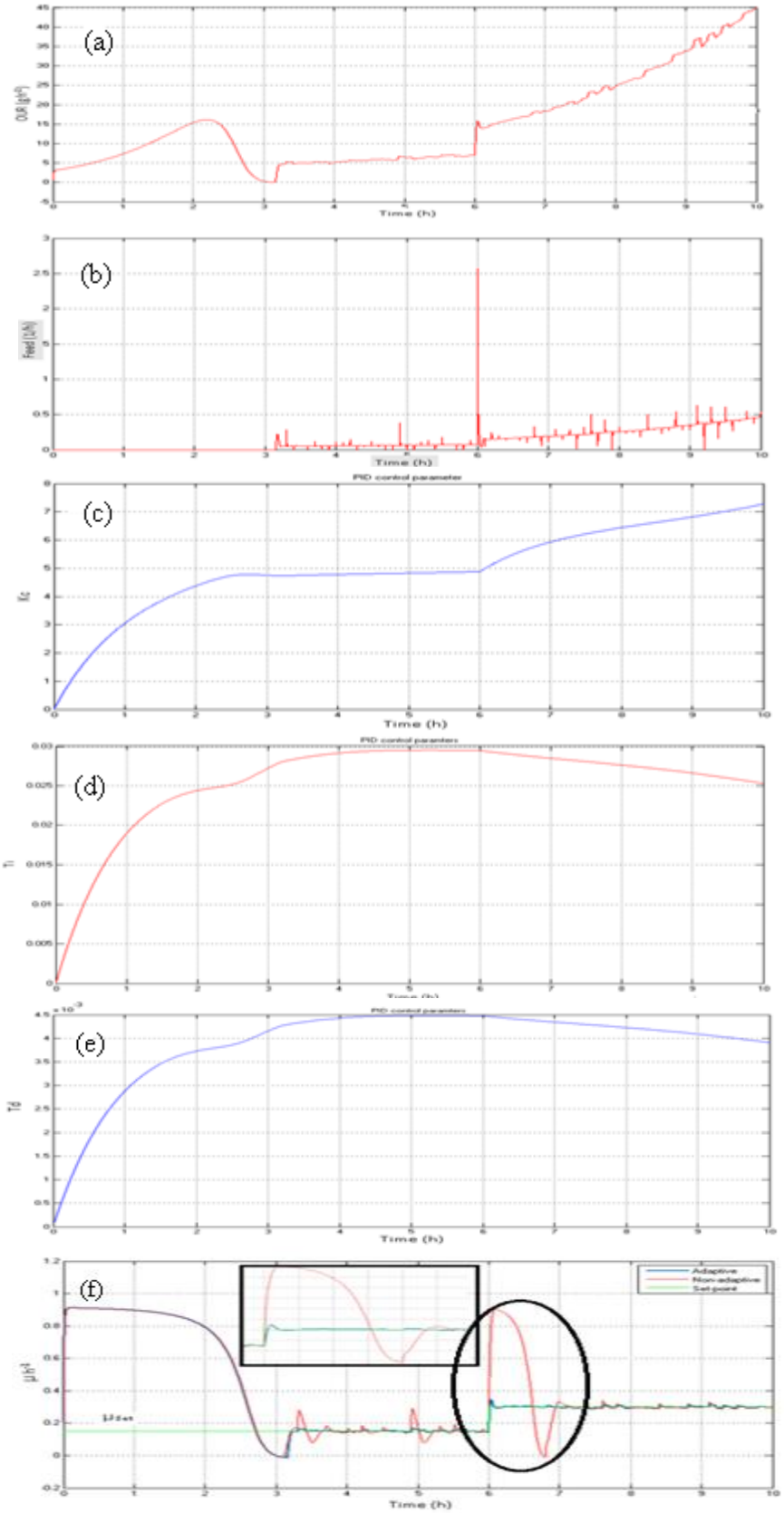

Figure 33. The simulation results show the dynamics of the process a)oxygen uptake rate (OUR), b) feeding rate (U_F), c) gain proportional (Kc), d) integration time constant (Ti), e) differentiation time constant (Td), f) specific growth rate (μ) with setpoint control change from (μ_{set} = 0.0501 h^{-1} to μ_{set}=0.3 h^{-1}) by automatic control system and simulation time is 6 (h)

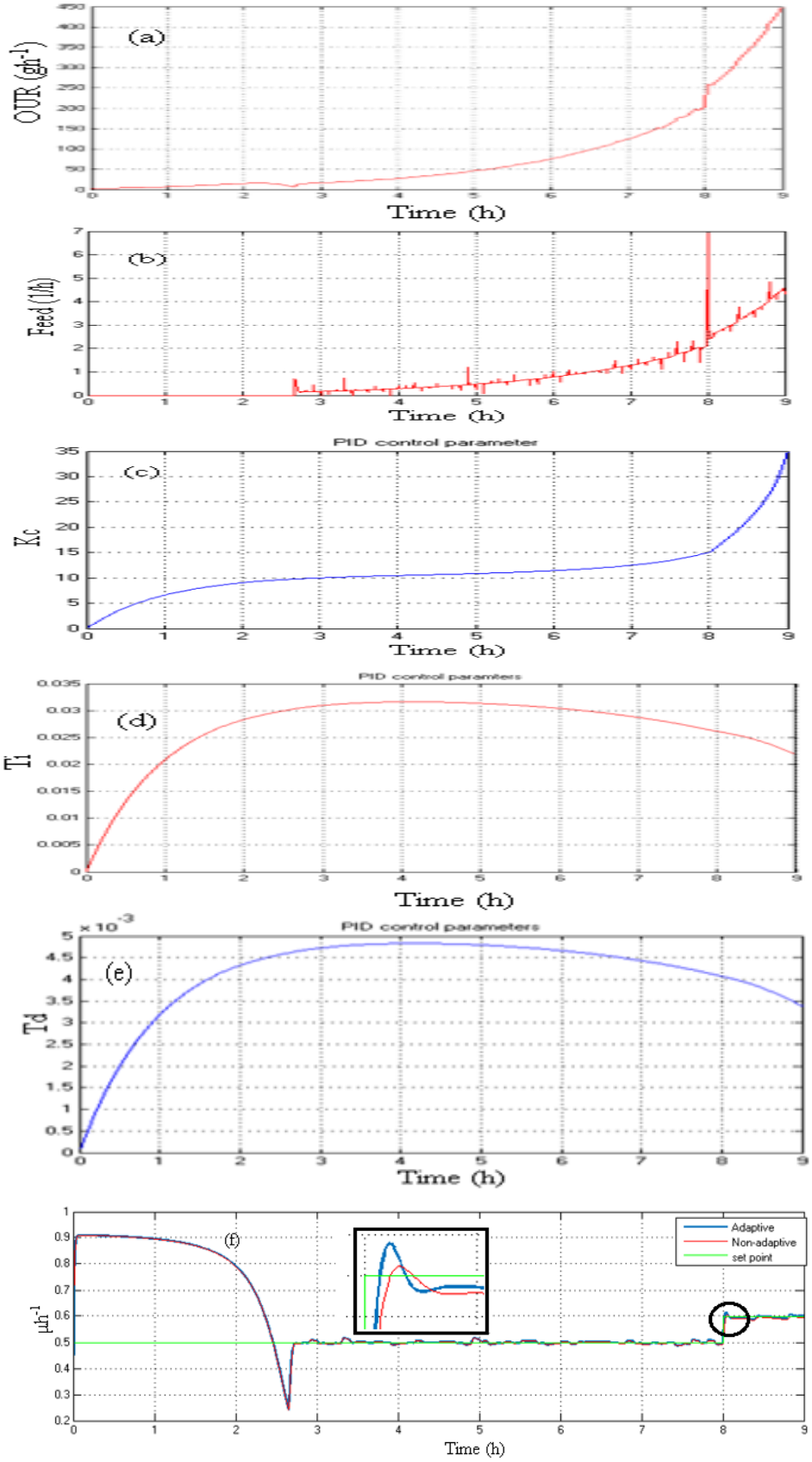

Figure 34 The simulation results show the dynamics of the process a)oxygen uptake rate (OUR), b) feeding rate (U_F), c) gain proportional (Kc), d) integration time constant (Ti), e) differentiation time constant (Td), f) specific growth rate (μ) with setpoint control change from (μ_{set} = 0.5 h^{-1} to μ_{set}=0.6 h^{-1}) by automatic control system and simulation time is 8 (h)

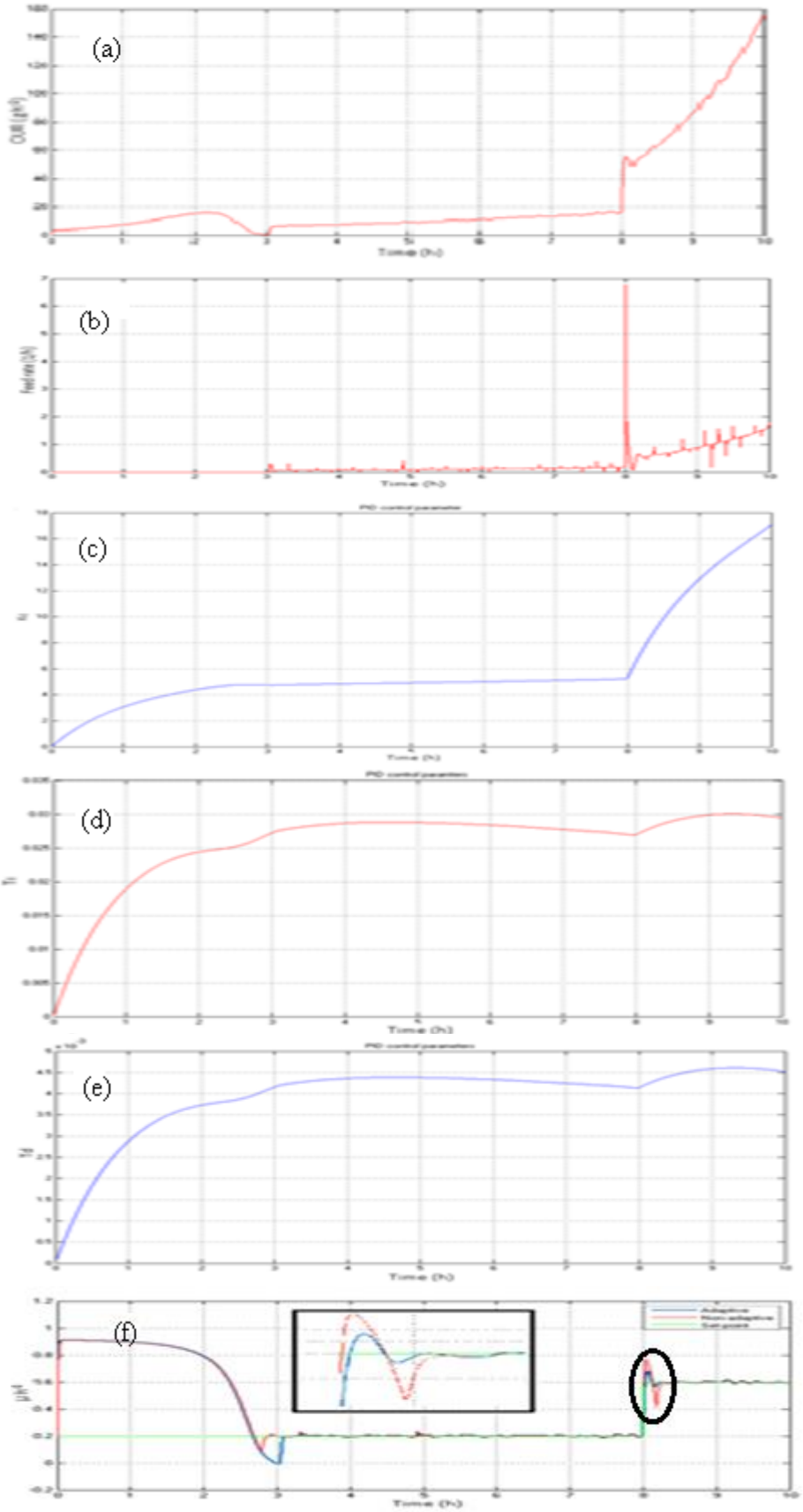

Figure 35. The simulation results show the dynamics of the process a)oxygen uptake rate (OUR), b) feeding rate (U_F), c) gain proportional (Kc), d) integration time constant (Ti), e) differentiation time constant (Td), f) specific growth rate (μ) with setpoint control change from (μ_{set} = 0.2 h^{-1} to μ_{set}=0.6 h^{-1}) by automatic control system and simulation time is 8 (h)

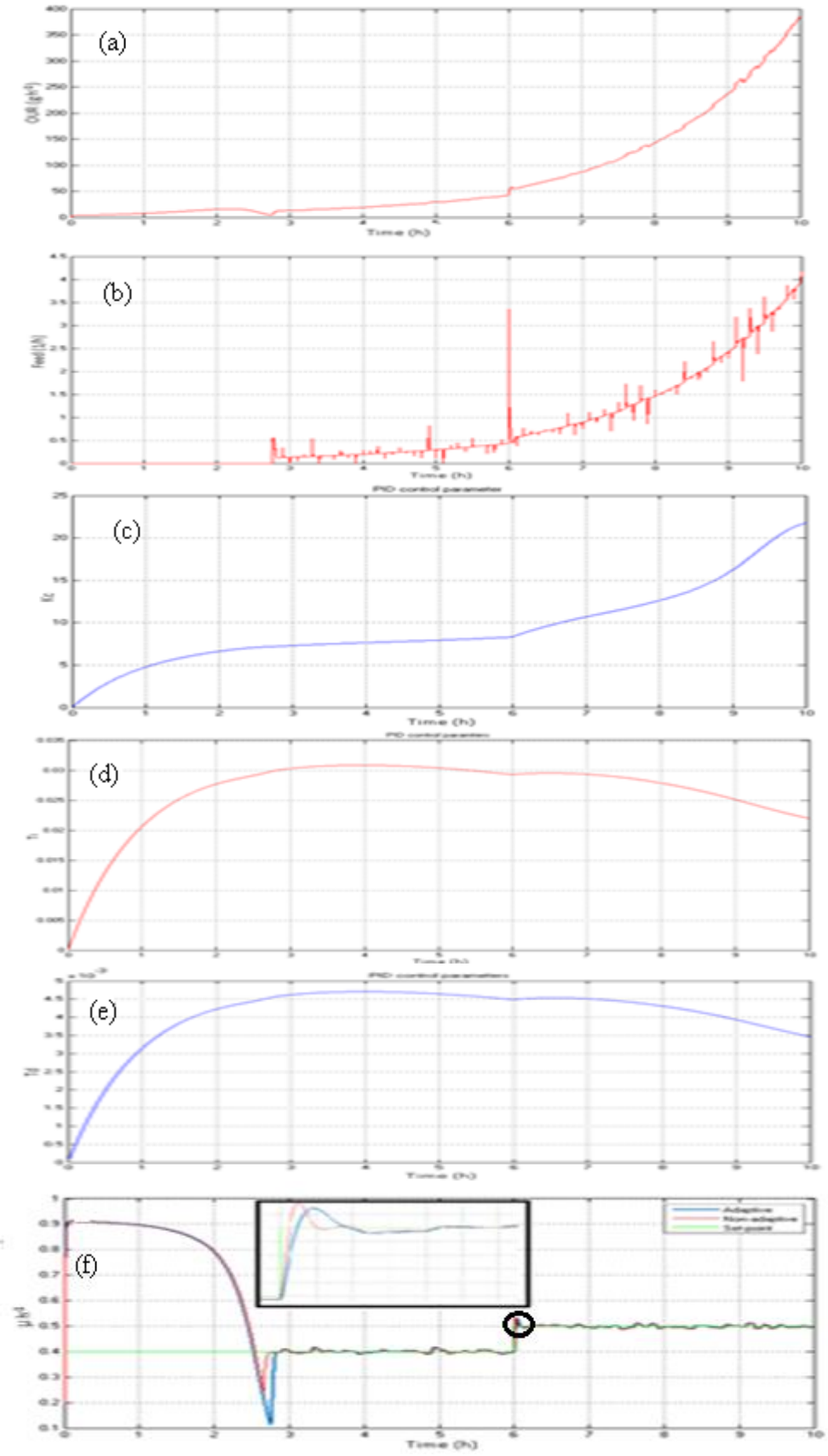

Figure 36. The simulation results show the dynamics of the process a)oxygen uptake rate (OUR), b) feeding rate (U_F), c) gain proportional (Kc), d) integration time constant (Ti), e) differentiation time constant (Td), f) specific growth rate (μ) with setpoint control change from (μ_{set} = 0.4 h^{-1} to μ_{set}=0.5 h^{-1}) by automatic control system and simulation time is 6(h)

Experiment 5: The set-point of specific growth rate(μ) was changed from μ_{set} = 0.0501 h^{-1} to μ_{set} = 0.1 h^{-1} and simulation time 6 (h) as shown in Figure 37. The overshoot and settling time of the adaptive system is decreased 37 %, decreased 28.75% compared to non-adaptive system respectively.

Table 13. PID controller model parameters

Model parameters (Initial 0.0501; Final 0.1)	Adaptive system	Non-adaptive system
Gain proportional (Kc)	5.545	8
Integration time constant (Ti)	0.023	0.035
Differentiation time constant (Td)	0.0035	0.0052

Experiment 6: The set-point of specific growth rate(μ) was changed from μ_{set} = 0.2 h^{-1} to μ_{set} = 0.5 h^{-1} and simulation time 6 (h) as shown in Figure 38. The overshoot and settling time of the adaptive system is decreased 17%, decreased 22.22% compared to non-adaptive system respectively.

Table 14. PID controller model parameters

Model parameters (Initial 0.2; Final 0.5)	Adaptive system	Non-adaptive system
Gain proportional (Kc)	14.49	20
Integration time constant (Ti)	0.02643	0.0288
Differentiation time constant (Td)	0.004115	0.00438

Experiment 7: The set-point of specific growth rate(μ) was changed from μ_{set} = 0.2 h^{-1} to μ_{set} = 0.3 h^{-1} and simulation time 6 (h) as shown in Figure 39. The overshoot and settling time of the adaptive system is decreased 75%, decreased 57.14% compared to non-adaptive system respectively.

Table 15. PID controller model parameters

Model parameters (Initial 0.2; Final 0.3)	Adaptive system	Non-adaptive system
Gain proportional (Kc)	7.613	15
Integration time constant (Ti)	0.0244	0.0281
Differentiation time constant (Td)	0.0038	0.0043

Experiment 8: The set-point of specific growth rate(μ) was changed from μ_{set} = 0.3 h^{-1} to μ_{set} = 0.6 h^{-1} and simulation time 8 (h) as shown in Figure 40. The overshoot and settling time of the adaptive system is decreased 31 %, decreased 50% compared to non-adaptive system respectively.

Table 16. PID controller model parameters

Model parameters (Initial 0.3; Final 0.6)	Adaptive system	Non-adaptive system
Gain proportional (Kc)	20.93	25
Integration time constant (Ti)	0.0264	0.0281
Differentiation time constant (Td)	0.0041	0.0043

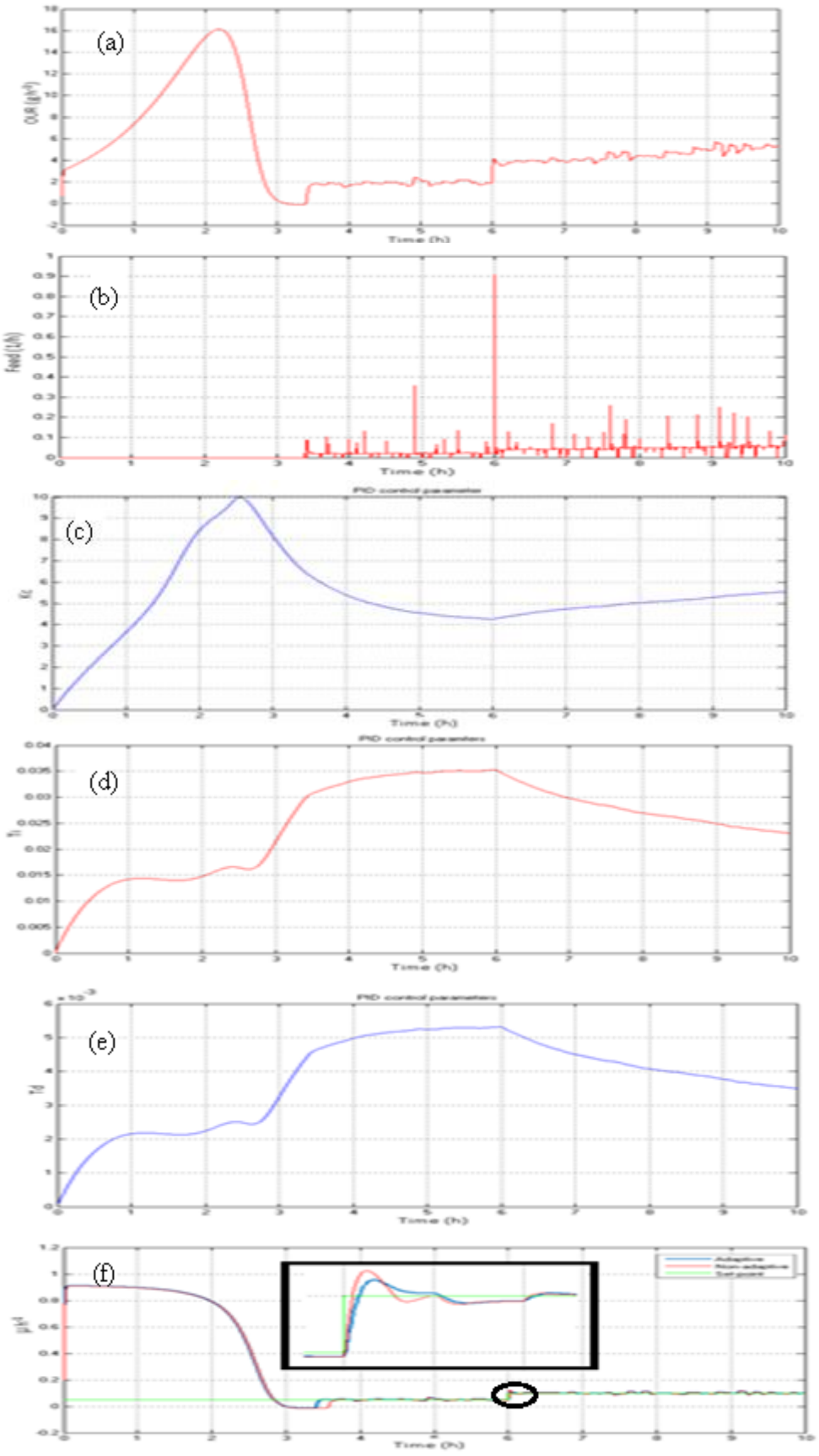

Figure 37. The simulation results show the dynamics of the process a)oxygen uptake rate (OUR), b) feeding rate (U_F), c) gain proportional (Kc), d) integration time constant (Ti), e) differentiation time constant (Td), f) specific growth rate (μ) with setpoint control change from (μ_{set} = 0.0501 h^{-1} to μ_{set}=0.1 h^{-1}) by automatic control system and simulation time is 6(h)

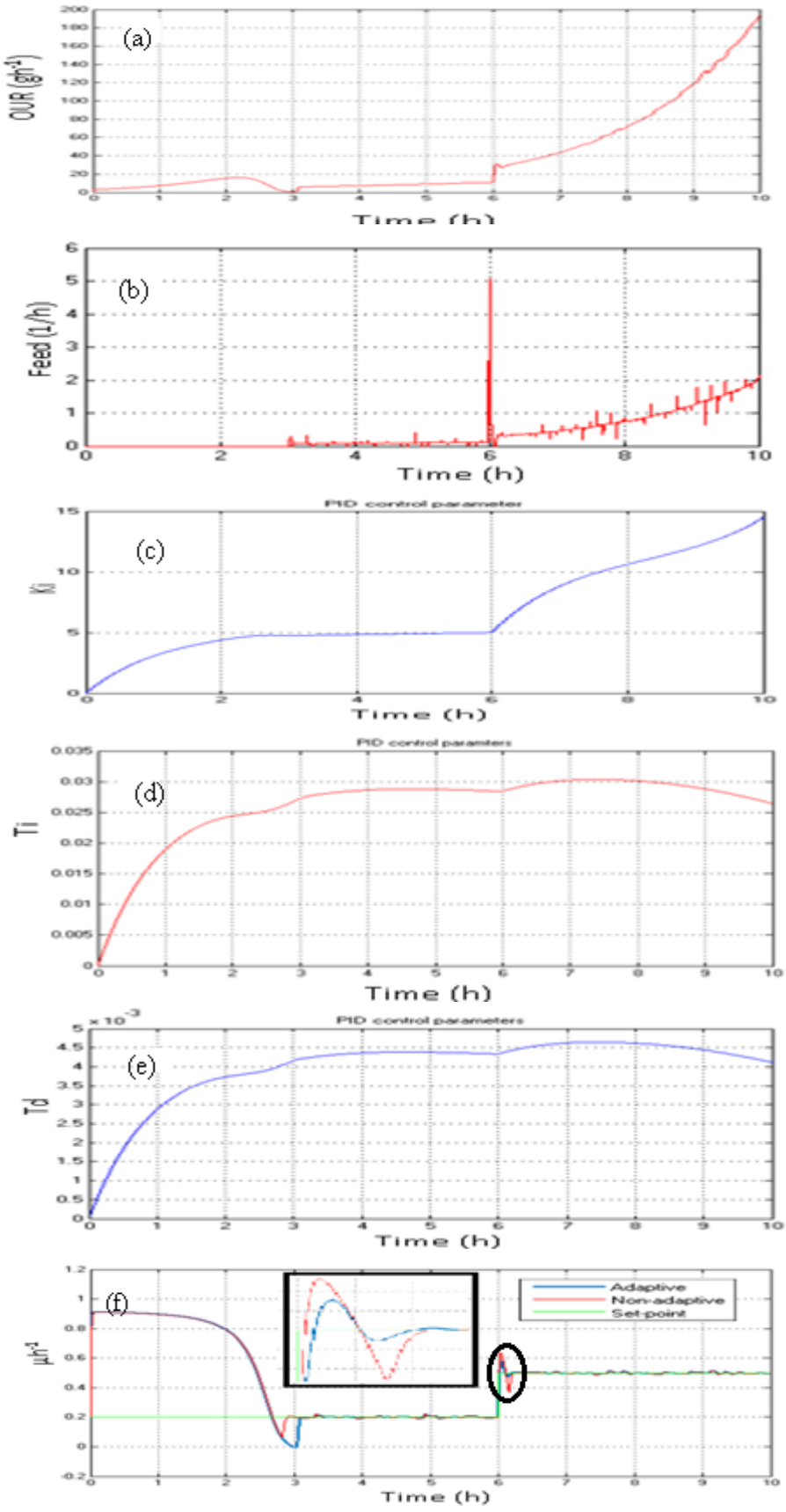

Figure 38. The simulation results show the dynamics of the process a)oxygen uptake rate (OUR), b) feeding rate (U_F), c) gain proportional (Kc), d) integration time constant (Ti), e) differentiation time constant (Td), f) specific growth rate (μ) with setpoint control change from (μ_{set} = 0.2 h^{-1} to μ_{set}=0.5 h^{-1}) by automatic control system and simulation time is 6(h)

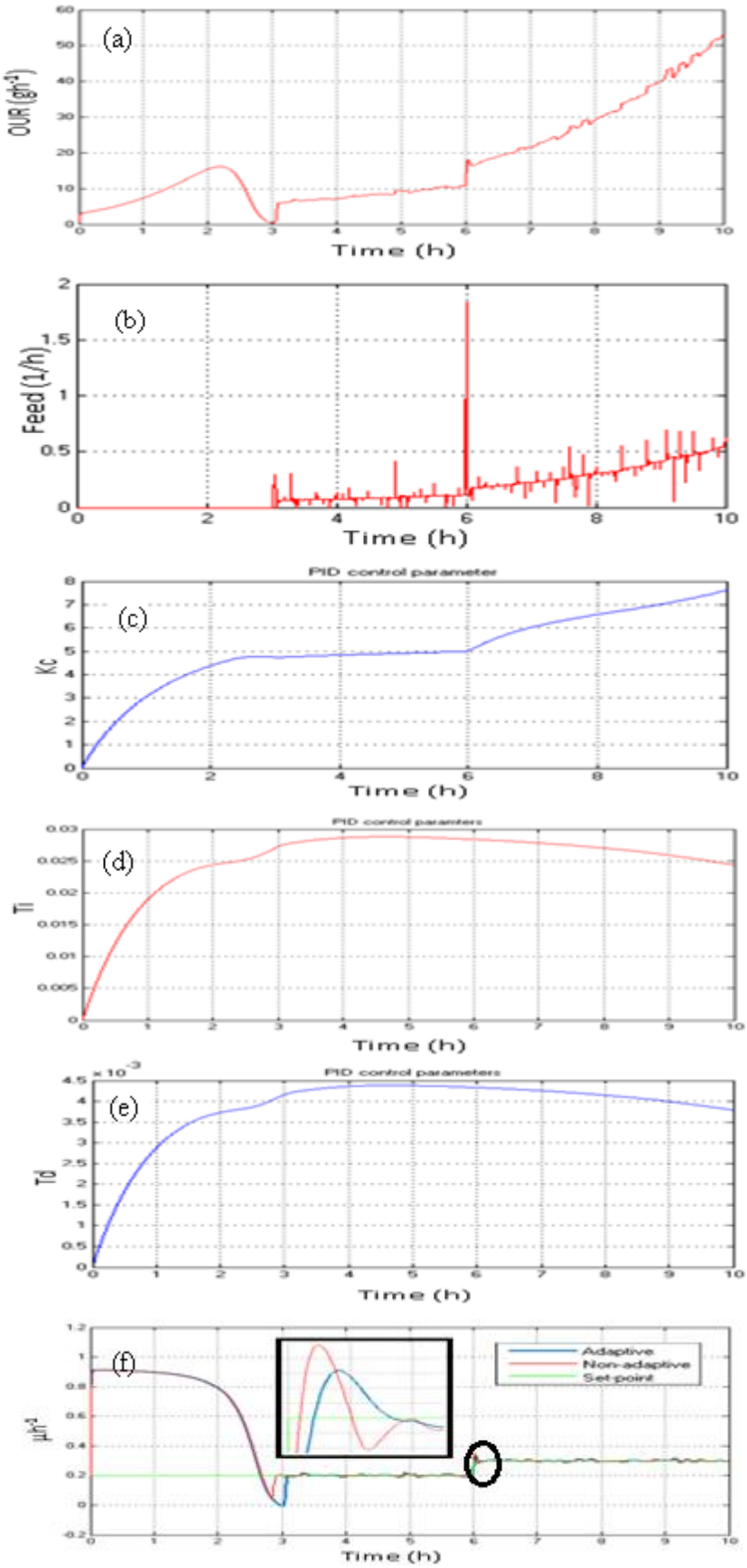

Figure 39. The simulation results show the dynamics of the process a)oxygen uptake rate (OUR), b) feeding rate (U_F), c) gain proportional (Kc), d) integration time constant (Ti), e) differentiation time constant (Td), f) specific growth rate (μ) with setpoint control change from (μ_{set} = 0.2 h^{-1} to μ_{set}=0.3 h^{-1}) by automatic control system and simulation time is 6(h)

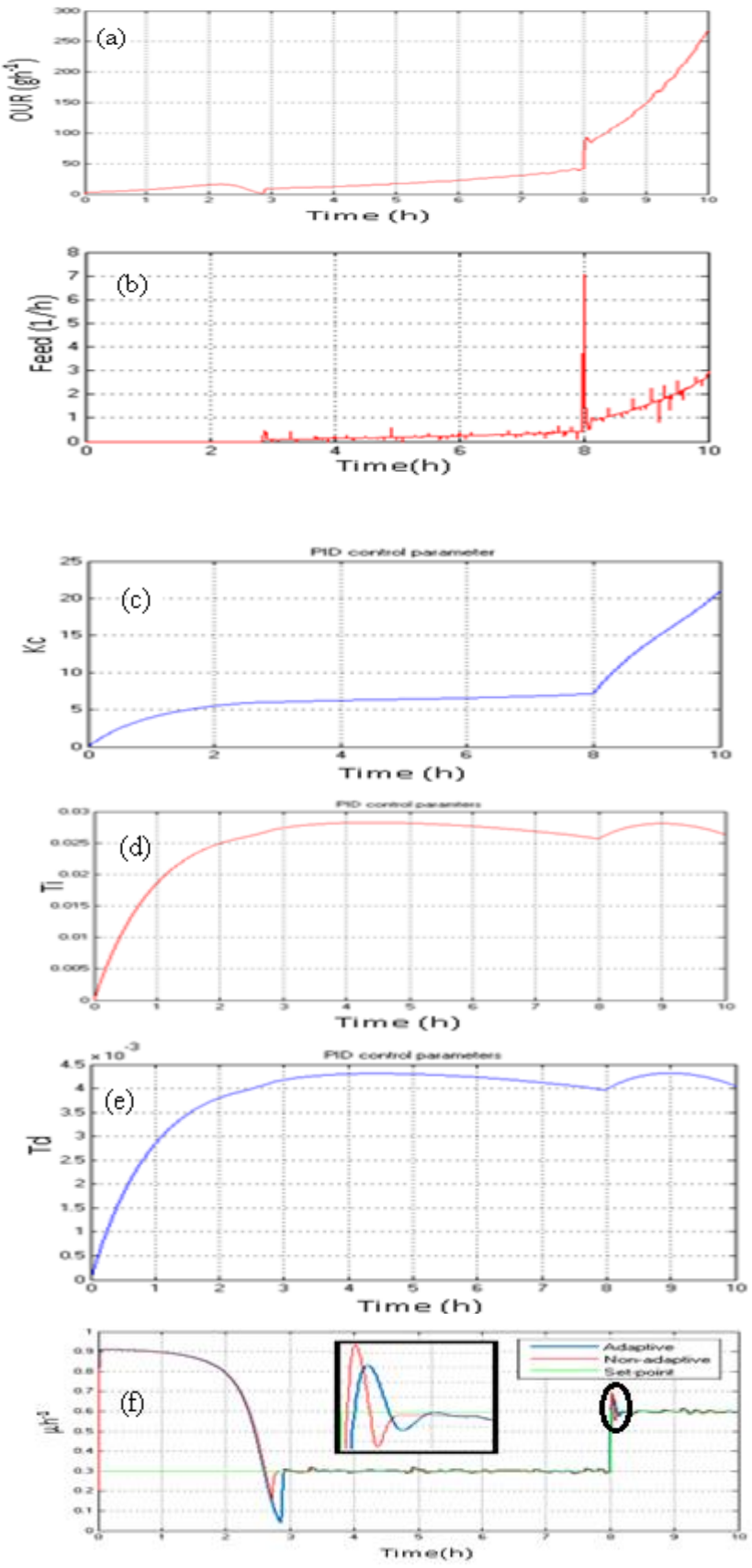

Figure 40. The simulation results show the dynamics of the process a)oxygen uptake rate (OUR), b) feeding rate (U_F), c) gain proportional (Kc), d) integration time constant (Ti), e) differentiation time constant (Td), f) specific growth rate (μ) with setpoint control change from (μ_{set} = 0.3 h^{-1} to μ_{set}=0.6 h^{-1}) by automatic control system and simulation time is 8(h)

Experiment 9: The set-point of specific growth rate(μ) was changed from $\mu_{set} = 0.3\ h^{-1}$ to $\mu_{set} = 0.1\ h^{-1}$ and simulation time 7 (h) as shown in Figure 41. The overshoot and settling time of the adaptive system is decreased 20 %, decreased 60% compared to non-adaptive system respectively.

Table 17. PID controller model parameters

Model parameters (Initial 0.3; Final 0.1)	Adaptive system	Non-adaptive system
Gain proportional (Kc)	12.5	10
Integration time constant (Ti)	0.0167	0.0282
Differentiation time constant (Td)	0.0025	0.0043

Experiment 10: The set-point of specific growth rate(μ) was changed from $\mu_{set} = 0.4\ h^{-1}$ to $\mu_{set} = 0.1\ h^{-1}$ and simulation time 7 (h) as shown in Figure 42. The overshoot and settling time of the adaptive system is decreased 45%, decreased 18.18 compared to non-adaptive system respectively.

Table 18. PID controller model parameters

Model parameters (Initial 0.4; Final 0.1)	Adaptive system	Non-adaptive system
Gain proportional (Kc)	6	15
Integration time constant (Ti)	0.0465	0.0304
Differentiation time constant (Td)	0.0070	0.0064

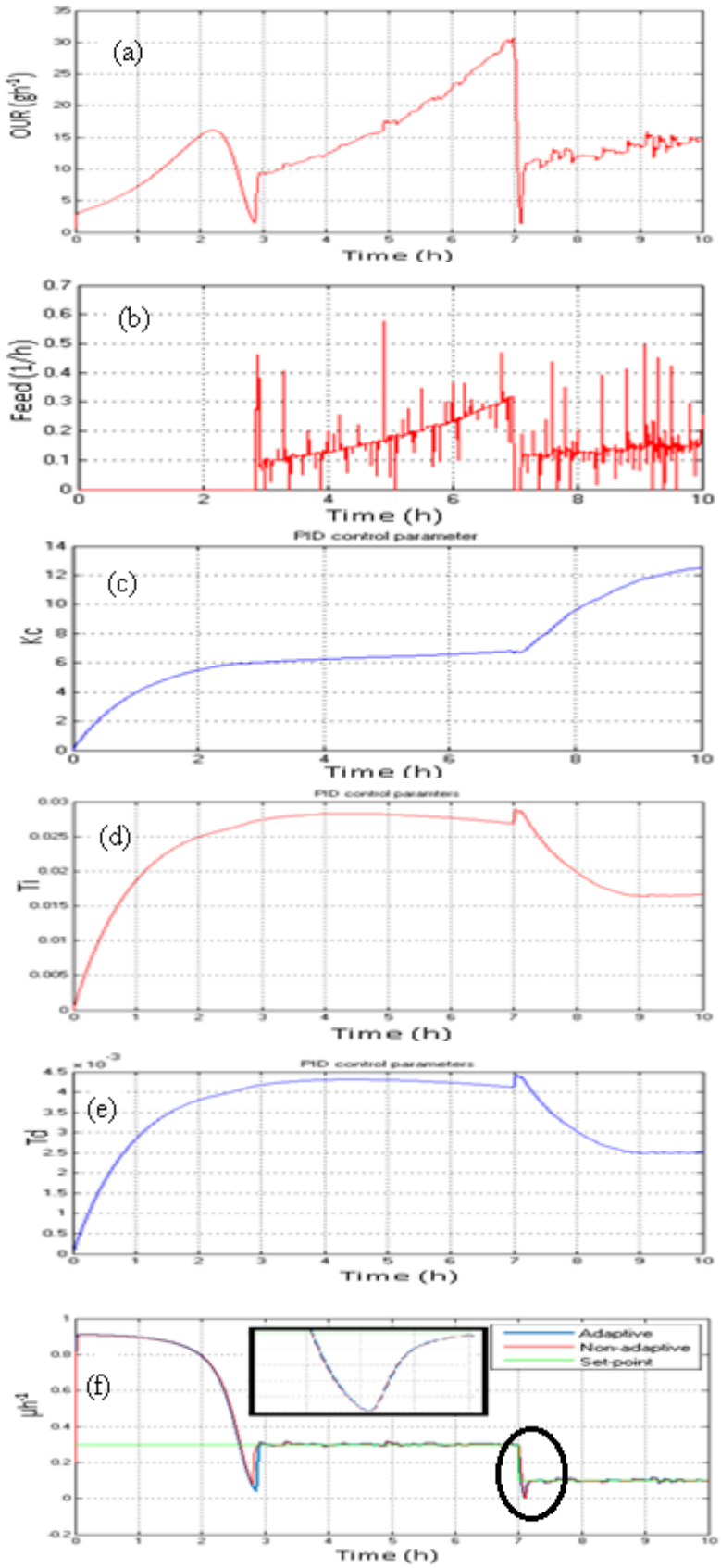

Figure 41. The simulation results show the dynamics of the process a)oxygen uptake rate (OUR), b) feeding rate (U_F), c) gain proportional (Kc), d) integration time constant (Ti), e) differentiation time constant (Td), f) specific growth rate (μ) with setpoint control change from (μ_{set} = 0.3 h^{-1} to μ_{set}=0.1 h^{-1}) by automatic control system and simulation time is 7(h)

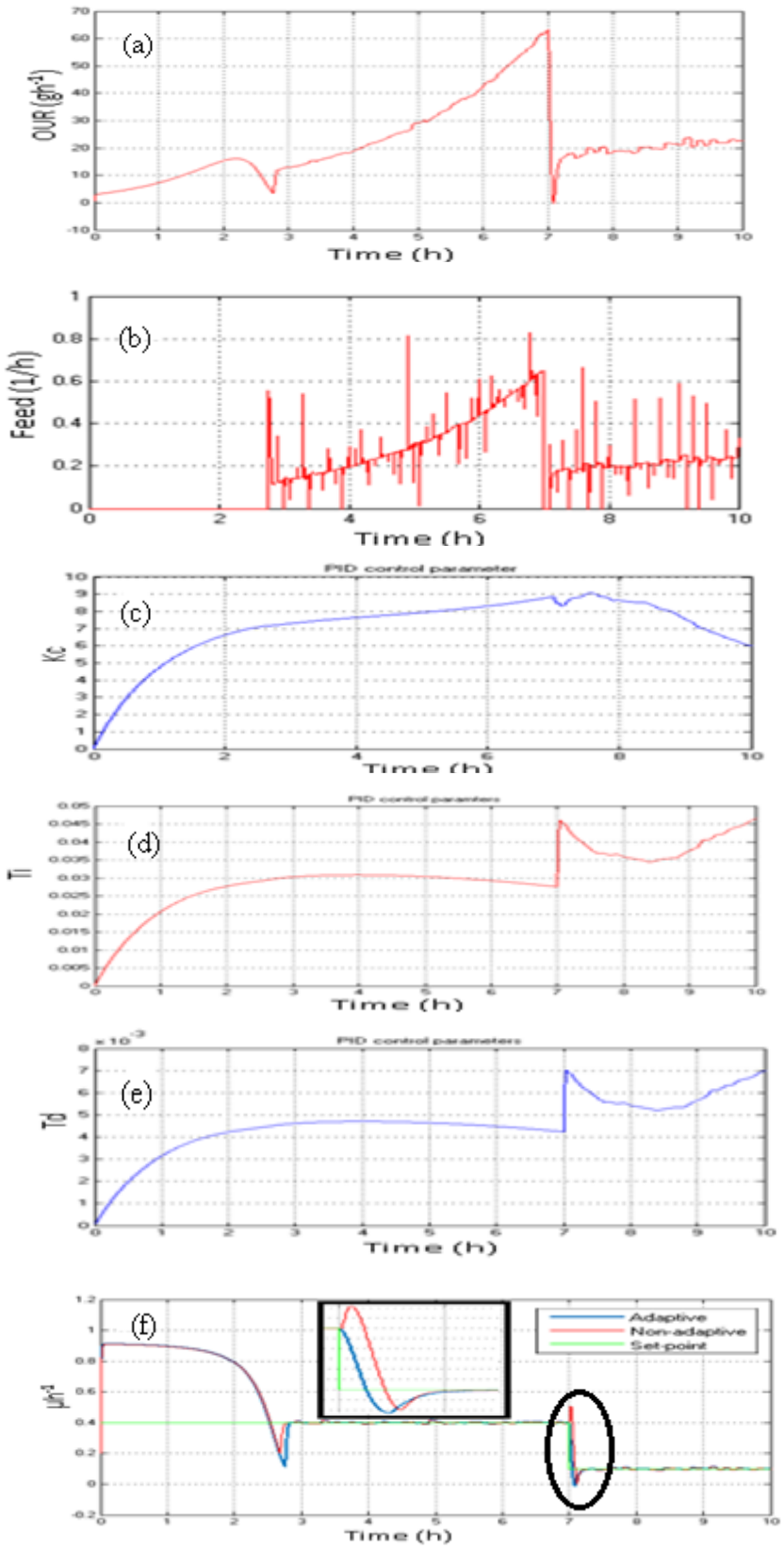

Figure 42. The simulation results show the dynamics of the process a)oxygen uptake rate (OUR), b) feeding rate (U_F), c) gain proportional (Kc), d) integration time constant (Ti), e) differentiation time constant (Td), f) specific growth rate (μ) with setpoint control change from (μ_{set} = 0.4 h^{-1} to μ_{set}=0.1 h^{-1}) by automatic control system and simulation time is 7(h)

CONCLUSIONS

1. Analysis of Fed-batch cultivation process an object of monitoring and control and analysis of mathematical models applied for modelling of fed-batch cultivation processes are presented.

2. MATLAB/SIMULINK model for simulation of E. coli fed-batch cultivation is developed and applied for investigation of the controlled process dynamics at various cultivation conditions.

3. PID controller gain scheduling algorithm is developed for controller adaptation to time-varying cultivation conditions. In the adaptation algorithm, the biomass specific growth rate and the oxygen uptake rate are used as gain scheduling variables.

4. MATLAB/SIMULINK models are developed for modelling of ordinary and the adaptive control systems. Simulation results of the investigated control systems performance under various cultivation conditions show that the adaptive control system outperforms the ordinary system. An overshoot of specific growth rate step response decreases in (11%-75%) and settling time decrease in (18.18%-67.63%).

5. The presented specific growth rate controller adaptation approach can be applied for the development of biomass growth control systems of various fed-batch cultivation processes.

REFERENCES

[1] J. K. Hedrick, 'Control of Nonlinear Dynamic Systems The University of California at Berkeley Department of Aerospace Engineering The University of Michigan at Ann Arbor', no. March, 2017.

[2] A. Esen, 'Chapter 1 - Introduction to Control System', *β-Glucosidases Biochem. Mol. Biol.*, pp. 1–14, 2003.

[3] O. T. Corporation, 'Biomass Production Growth Unit', vol. 26, no. 2, pp. 289–298, 2000.

[4] K. J. Blose, J. T. Krawiec, J. S. Weinbaum, and D. A. Vorp, *Bioreactors for tissue engineering purposes*. Elsevier Inc., 2014.

[5] S. Ali, A. Rafique, M. Ahmed, and S. Sakandar, 'Different Type of Industrial Fermentors and Their Associated Operations for the Mass Production of Metabolite', *Eur. J. Pharm. Med. Res. www.ejpmr.com*, vol. 5, no. 5, pp. 109–119, 2018.

[6] A.-N. A. Zohri, S. W. Ragab, M. I. Mekawi, and O. A. A. Mostafa, 'Comparison Between Batch, Fed-Batch, Semi-Continuous and Continuous Techniques for Bio-Ethanol Production from a Mixture of Egyptian Cane and Beet Molasses', *Egypt. Sugar J.*, vol. 9, no. September, pp. 89–111, 2017.

[7] S. M. Woodside, B. D. Bowen, and J. M. Piret, 'Mammalian cell retention devices for stirred perfusion bioreactors.', *Cytotechnology*, vol. 28, no. 1–3, pp. 163–75, 1998.

[8] M. Björklund, 'Cell size homeostasis: Metabolic control of growth and cell division', *Biochim. Biophys. Acta - Mol. Cell Res.*, vol. 1866, no. 3, pp. 409–417, 2019.

[9] E. Krichen, J. Harmand, M. Torrijos, J. J. Godon, N. Bernet, and A. Rapaport, 'High biomass density promotes density-dependent microbial growth rate', *Biochem. Eng. J.*, vol. 130, pp. 66–75, 2018.

[10] B. Liu *et al.*, 'Modelling the effects of post-heading heat stress on biomass growth of winter wheat', *Agric. For. Meteorol.*, vol. 247, no. March, pp. 476–490, 2017.

[11] P. Prachanurak, C. Chiemchaisri, W. Chiemchaisri, and K. Yamamoto, 'Modelling of biofilm growth for photosynthetic biomass production in a pipe-overflow recirculation bioreactor', *Biochem. Eng. J.*, vol. 142, no. November 2018, pp. 50–57, 2019.

[12] D. E. Berthold, K. G. Shetty, K. Jayachandran, H. D. Laughinghouse, and M. Gantar, 'Enhancing algal biomass and lipid production through bacterial co-culture', *Biomass and Bioenergy*, vol. 122, no. January, pp. 280–289, 2019.

[13] N. Wang *et al.*, 'Modelling maize phenology, biomass growth and yield under contrasting temperature conditions', *Agric. For. Meteorol.*, vol. 250–251, no. September 2017, pp. 319–329, 2018.

[14] V. Astolfi *et al.*, 'Operation of a fixed-bed bioreactor in batch and fed-batch modes for production of inulinase by solid-state fermentation', *Biochem. Eng. J.*, vol. 58–59, no. 1, pp. 39–49, 2011.

[15] J. Gonciarz, A. Kowalska, and M. Bizukojc, 'Application of microparticle-enhanced cultivation to increase the access of oxygen to Aspergillus terreus ATCC 20542 mycelium and intensify lovastatin biosynthesis in batch and continuous fed-batch stirred tank bioreactors', *Biochem. Eng. J.*, vol. 109, pp. 178–188, 2016.

[16] S. Marques, C. T. Matos, F. M. Gírio, J. C. Roseiro, and J. A. L. Santos, 'Lactic acid production from recycled paper sludge: Process intensification by running fed-batch into a membrane-recycle bioreactor', *Biochem. Eng. J.*, vol. 120, pp. 63–72, 2017.

[17] C. Retamal, L. Dewasme, A. L. Hantson, and A. Vande Wouwer, 'Parameter estimation of a dynamic model of Escherichia coli fed-batch cultures', *Biochem. Eng. J.*, vol. 135, pp. 22–35, 2018.

[18] I. I. K. Veloso, K. C. S. Rodrigues, J. L. S. Sonego, A. J. G. Cruz, and A. C. Badino, 'Fed-batch ethanol fermentation at low temperature as a way to obtain highly concentrated alcoholic wines: Modeling and optimization', *Biochem. Eng. J.*, vol. 141, no. October 2018, pp. 60–70, 2019.

[19] M. Laureni *et al.*, 'Biomass segregation between biofilm and flocs improves the control of nitrite-oxidizing bacteria in mainstream partial nitritation and anammox processes', *Water Res.*, vol. 154, pp. 104–116, 2019.

[20] D. Ehgartner *et al.*, 'Controlling the specific growth rate via biomass trend regulation in filamentous fungi bioprocesses', *Chem. Eng. Sci.*, vol. 172, pp. 32–41, 2017.

[21] M. Navrátil, A. Norberg, L. Lembrén, and C. F. Mandenius, 'On-line multi-analyzer monitoring of biomass, glucose and acetate for growth rate control of a Vibrio cholerae fed-batch cultivation', *J. Biotechnol.*, vol. 115, no. 1, pp. 67–79, 2005.

[22] M. Jenzsch, S. Gnoth, M. Beck, M. Kleinschmidt, R. Simutis, and A. Lübbert, 'Open-loop control of the biomass concentration within the growth phase of recombinant protein production processes', *J. Biotechnol.*, vol. 127, no. 1, pp. 84–94, 2006.

[23] M. Müller, W. Meusel, U. Husemann, G. Greller, and M. Kraume, 'Application of heat compensation calorimetry to an E. coli fed-batch process', *J. Biotechnol.*, vol. 266, no. July 2017, pp. 133–143, 2018.

[24] R. Wang, P. Unrean, and C. J. Franzén, 'Model-based optimization and scale-up of multi-feed simultaneous saccharification and co-fermentation of steam pre-treated lignocellulose enables high gravity ethanol production', *Biotechnol. Biofuels*, vol. 9, no. 1, pp. 1–13, 2016.

[25] V. Bertrand *et al.*, 'Proteomic analysis of micro-scale bioreactors as scale-down model for a mAb producing CHO industrial fed-batch platform', *J. Biotechnol.*, vol. 279, no. April, pp. 27–36, 2018.

[26] N. Patel and N. Padhiyar, 'Multi-objective dynamic optimization study of fed-batch bio-reactor', *Chem. Eng. Res. Des.*, vol. 119, pp. 160–170, 2017.

[27] J. Lipovsky, P. Patakova, L. Paulova, T. Pokorny, M. Rychtera, and K. Melzoch, 'Butanol production by Clostridium pasteurianum NRRL B-598 in continuous culture compared to batch and fed-batch systems', *Fuel Process. Technol.*, vol. 144, pp. 139–144, 2016.

[28] D. Levisauskas, 'Inferential control of the specific growth rate in fed-batch cultivation processes', *Biotechnol. Lett.*, vol. 23, no. 15, pp. 1189–1195, 2001.

[29] M. Jenzsch, R. Simutis, and A. Luebbert, 'Generic model control of the specific growth rate in recombinant Escherichia coli cultivations', *J. Biotechnol.*, vol. 122, no. 4, pp. 483–493, 2006.

[30] D. Levišauskas, R. Simutis, and V. Galvanauskas, 'Adaptive set-point control system for microbial', vol. 21, no. 2, pp. 153–165, 2016.

[31] J. L. Snoep, M. Mrwebi, J. M. Schuurmans, J. M. Rohwer, and M. J. T. Teixeira de Mattor, 'Control of specific growth rate in Saccharomyces cerevisiae', *Microbiology*, vol. 155, no. 5, pp. 1699–1707, 2009.

[32] M. M. Schuler and I. W. Marison, 'Real-time monitoring and control of microbial bioprocesses with focus on the specific growth rate: Current state and perspectives', *Appl. Microbiol. Biotechnol.*, vol. 94, no. 6, pp. 1469–1482, 2012.

[33] I. Rocha, A. Veloso, S. Carneiro, E. Ferreira, and R. Costa, *Implementation of a specific rate controller in a fed-batch E. coli fermentation*, vol. 17, no. 1 PART 1. IFAC, 2008.

[34] 'Bioreactor Monitoring & Control Bioreactor Monitoring & Control Bioreactor Monitoring & Control Bioreactor Monitoring & Control'.

[35] S. G. Anavatti, F. Santoso, and M. A. Garratt, 'Progress in ACSs: past, present, and future', no. October, pp. 1–8, 2016.

[36] D. Levisauskas, R. Simutis, D. Borvitz, and A. Lübbert, 'Automatic control of the specific

growth rate in fed-batch cultivation processes based on an exhaust gas analysis', *Bioprocess Eng.*, vol. 15, no. 3, pp. 145–150, 1996.

[37] M. Shahrokhi and A. Zomorrodi, 'Comparison of Tuning Methods of Pid Controller', *Dep. Chem. Pet. Eng. Sharif Univ. Technol.*, pp. 1–2, 2013.

[38] P. I. N. Vinegar, 'the Analyst. the Analyst ', vol. 105, no. 1249, pp. 517–519, 1909.

[39] Donatas Levisauskas (2008), 'Alignment of automatic control systems', publisher of Vilnius pedagogical university.

APPENDICES

Number 1. Mathematical model used in the experiment

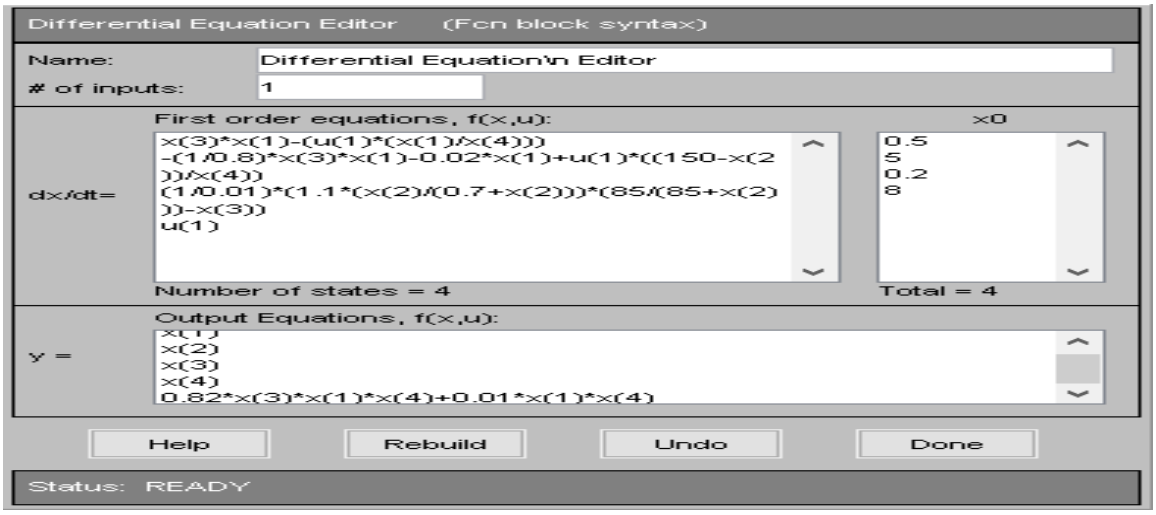

Number 2. Developing and testing model performance using MATLAB/SIMULINK tool

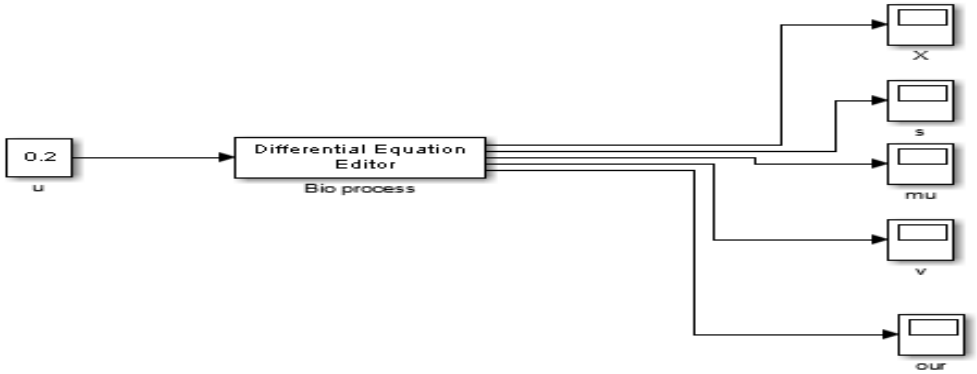

Number 3. Testing of model performance using feed-forward control

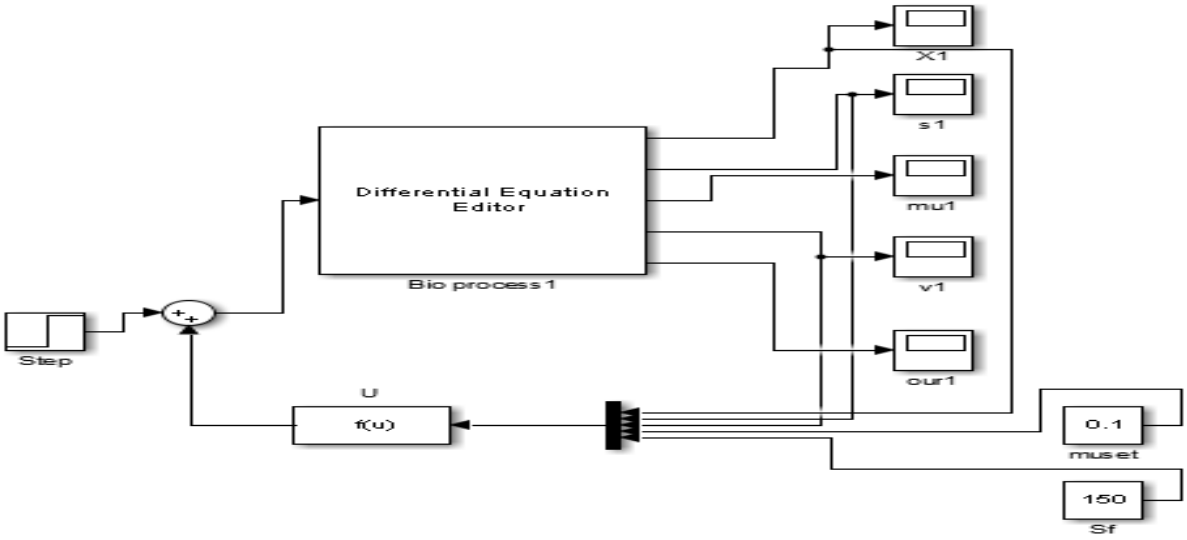

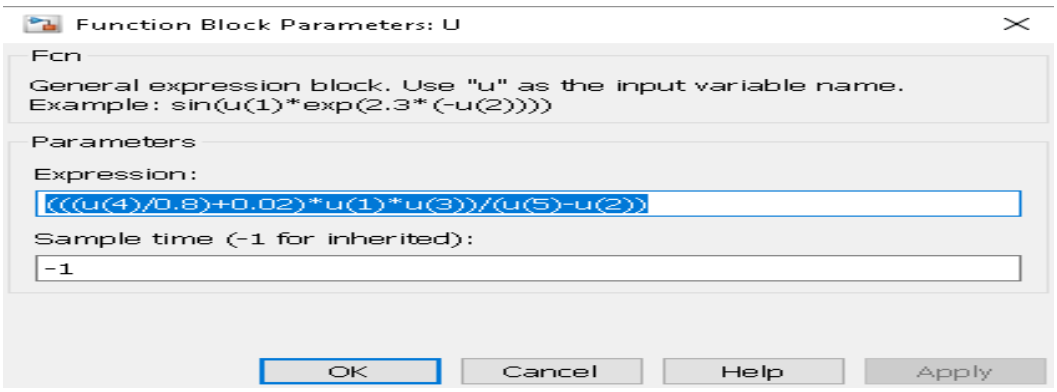

Number 4. The reaction curve (model performance of feed -forward control) and experimental curve of the model used for investigation of the process dynamic parameters.

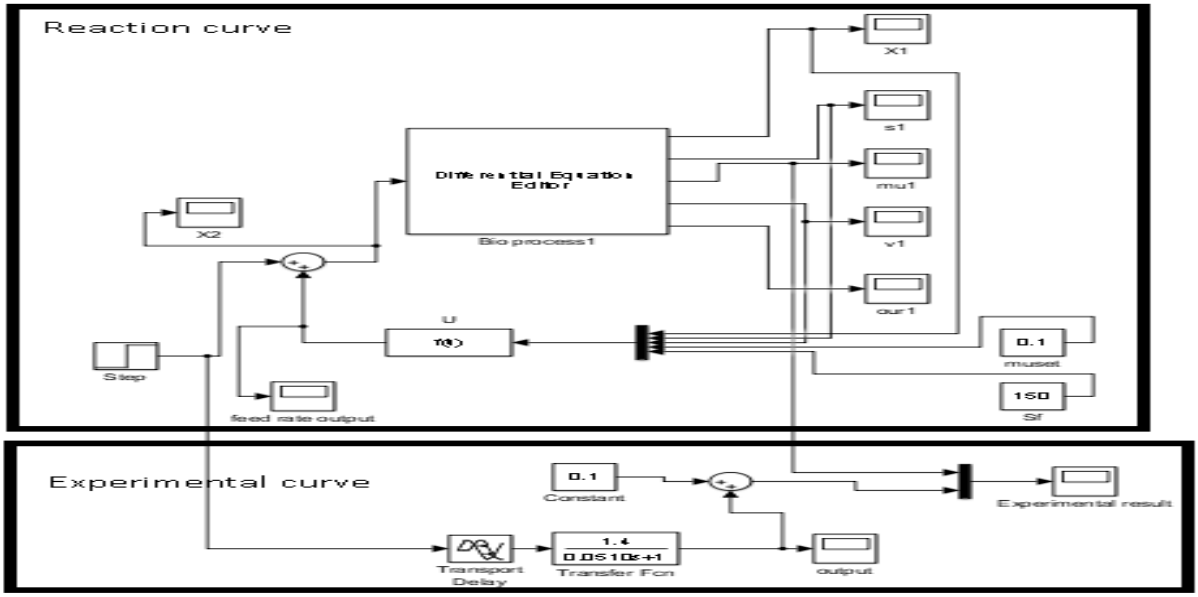

Number 5. The least squares method in a MATLAB / SIMULINK environment. A resizer program was found by counting the gain co-efficient

```
%function main
clc, clear
E_number=6;
N=1:1:E_number;
A_number=6;
x(:1)=[1 1 1 1 1 1]';
x(:2)=[4.6304 5.1194 5.6578 6.2529 7.6367 12.5927]';
x(:3)=[21.4406 26.2082 32.0107 39.0987 58.3191 158.5760]';
F=[x(:1),x(:2),x(:2).^2];
%K
Ye=[2.37 2.14 1.87 1.7 1.4 0.89]';
A=(inv(F'*F))*F'*Ye
Ym=F*A;
figure(1)
plot(N,Ym,'x',N,Ye,'o');
```

Number 6. The MATLAB / Simulink program calculates the values by calculating the K-factor

```
%K=a0+a1(OUR)+a2(OUR)2
clc,clear
%OUR = x(:3)
x(:3)=[4.6304 5.1194 5.6578 6.2529 7.6367 12.5927]';
a0= 4.8751;
a1=-0.6863;
a2=0.0294;
k=a0+(a1*(x(:3)))+(a2*(x(:3)).^2)
```

Number 7. The least squares method in a MATLAB / SIMULINK environment. A resizer program was found by counting the time constant

```
%function main
clc, clear
E_number=6;
N=1:1:E_number;
A_number=6;
x(:1)=[1 1 1 1 1 1]';
x(:2)=[4.6304 5.1194 5.6578 6.2529 7.6367 12.5927]';
x(:3)=[21.4406 26.2082 32.0107 39.0987 58.3191 158.5760]';
F=[x(:1),x(:2),x(:2).^2];
%T
Ye=[0.0975 0.0869 0.0689 0.0627 0.0510 0.0408]';
A=(inv(F'*F))*F'*Ye
Ym=F*A;
figure(1)
plot(N,Ym,'x',N,Ye,'o');
```

Number 8. The MATLAB / Simulink program calculates the values by calculating the T-factor

```
%T=a0+a1(OUR)+a2(OUR)2
clc,clear
%OUR = x(:3)
x(:3)=[4.6304 5.1194 5.6578 6.2529 7.6367 12.5927]';
a0= 0.2381;
a1=-0.0400;
a2=0.0020;
T=a0+(a1*(x(:3)))+(a2*(x(:3)).^2)
```

Number 9. The least squares method in a MATLAB / SIMULINK environment. A resizer program was found by counting the time delay

```
%function main
clc, clear
E_number=6;
N=1:1:E_number;
```

```
A_number=6;
x(:1)=[1 1 1 1 1 1]';
x(:2)=[4.6304 5.1194 5.6578 6.2529 7.6367 12.5927]';
x(:3)=[21.4406 26.2082 32.0107 39.0987 58.3191 158.5760]';
F=[x(:1),x(:2),x(:2).^2];
%τ
Ye=[0.0099 0.0095 0.0087 0.0077 0.0066 0.0056]';
A=(inv(F'*F))*F'*Ye
Ym=F*A;
figure(1)
plot(N,Ym,'x',N,Ye,'o');
```

Number 10. The MATLAB / Simulink program calculates the values by calculating the τ-factor

```
%τ=a0+a1(OUR)+a2(OUR)2
clc,clear
%OUR = x(:3)
x(:3)=[4.6304 5.1194 5.6578 6.2529 7.6367 12.5927]';
a0=0.0196;
a1=-0.0026;
a2=1.2042e-04;
τ=a0+(a1*(x(:3)))+(a2*(x(:3)).^2)
```

Number 11. The "μ" controller adaptation algorithm based on the expert "IF-THEN" rules

```
function [K_pr,T_pr,Tau_pr] = fcn(u)
mu=u(1);
our=u(2);
y_1=0;
y_2=0;
y_3=0;
if (0.05 < mu && mu < 0.15 )
    y_1=4.8751+(-0.6863)*(our)+(0.0294)*(our)^2;
    y_2=0.2381+(-0.0400)*(our)+(0.0020)*(our)^2;
    y_3=0.01961+(-0.0026)*(our)+(1.2052e-04)*(our)^2;
   elseif  (0.15 < mu && mu < 0.25)
    y_1=3.0068+(-0.1449)*(our)+(0.0022)*(our)^2;
    y_2=0.1403+(-0.0069)*(our)+(1.0824e-04)*(our)^2;
    y_3=0.0135+(-1.4326e-04)*(our)+(1.0348e-06)*(our)^2;
   elseif (0.25 < mu && mu < 0.35)
    y_1=1.8093+(-0.0332)*(our)+(1.7472e-04)*(our)^2;
    y_2=0.1062+(-0.0019)*(our)+(1.0497e-05)*(our)^2;
    y_3=0.0129+(-5.0891e-05)*(our)+(3.4919e-08)*(our)^2;
   elseif (0.35 < mu && mu < 0.45)
     y_1=1.4311+(-0.0169)*(our)+(6.2045e-05)*(our)^2;
     y_2=0.1127+(-0.0013)*(our)+(4.7972e-06)*(our)^2;
     y_3=0.0143+(-5.5698e-05)*(our)+(1.4166e-07)*(our)^2;
```

```
    elseif (0.45 < mu && mu < 0.55)
     y_1=0.9445+(-0.0057)*(our)+(1.0065e-05)*(our)^2;
     y_2=0.1038+(-5.6808e-04)*(our)+(1.0274e-06)*(our)^2;
     y_3=0.0143+(-2.1297e-05)*(our)+(1.6875e-08)*(our)^2;
    elseif (0.55 < mu && mu < 0.65)
     y_1=0.5151+(-0.0010)*(our);
     y_2=0.0890+(-1.3060e-04)*(our);
     y_3=0.0150+(-1.8537e-05)*(our);
end
K_pr=y_1;
T_pr=y_2;
Tau_pr=y_3;
```

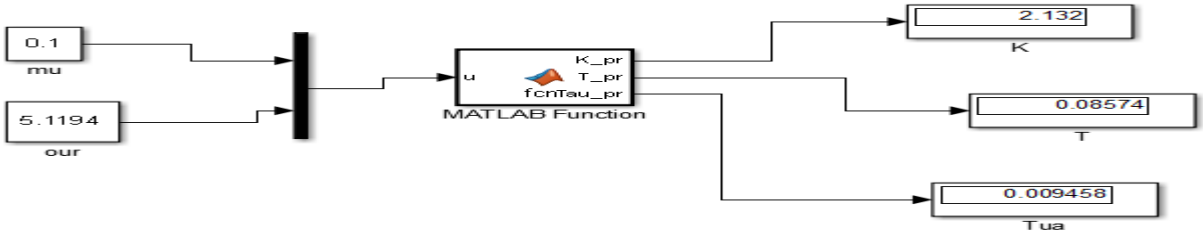

Number 12. PID controller gain scheduling algorithm by using Cohen and coon adjustment parameter

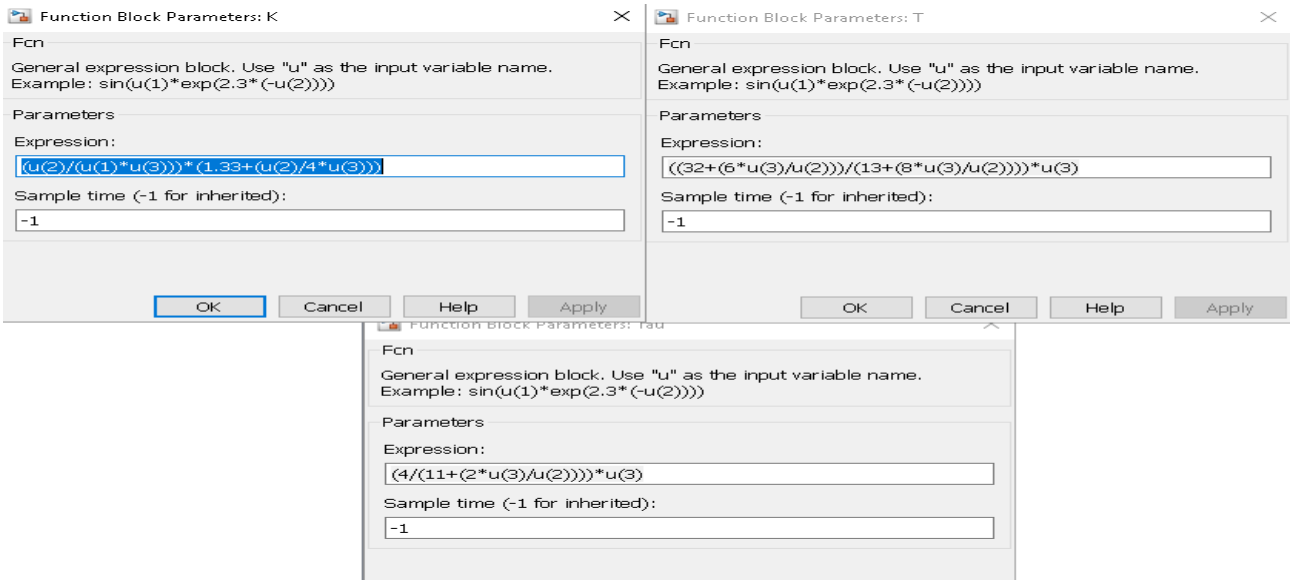

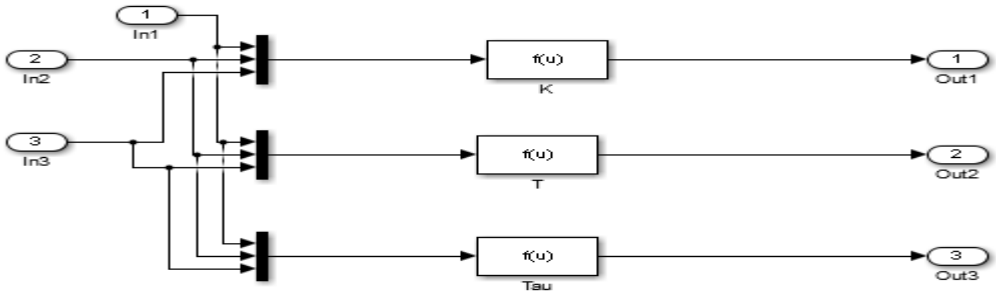

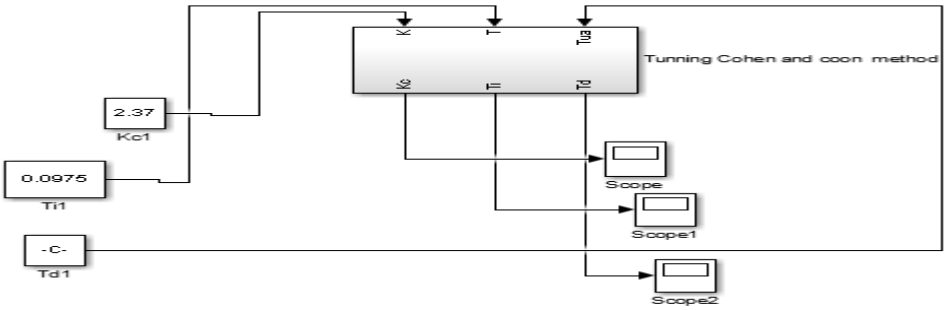

Number 13. Simulation of ordinary control system

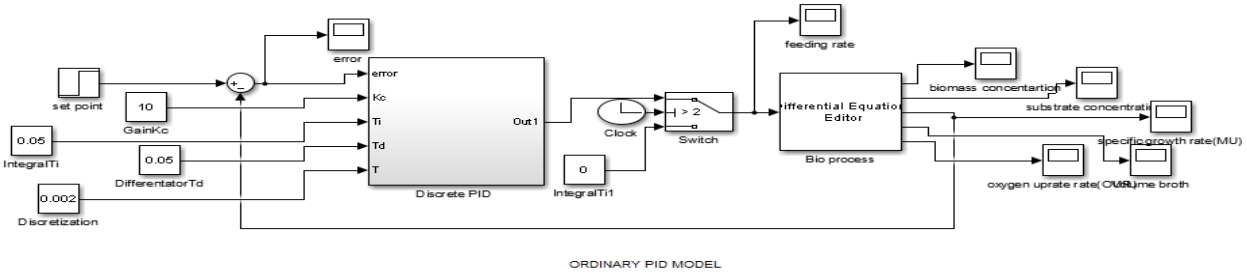

Number 14. Simulation of ACS

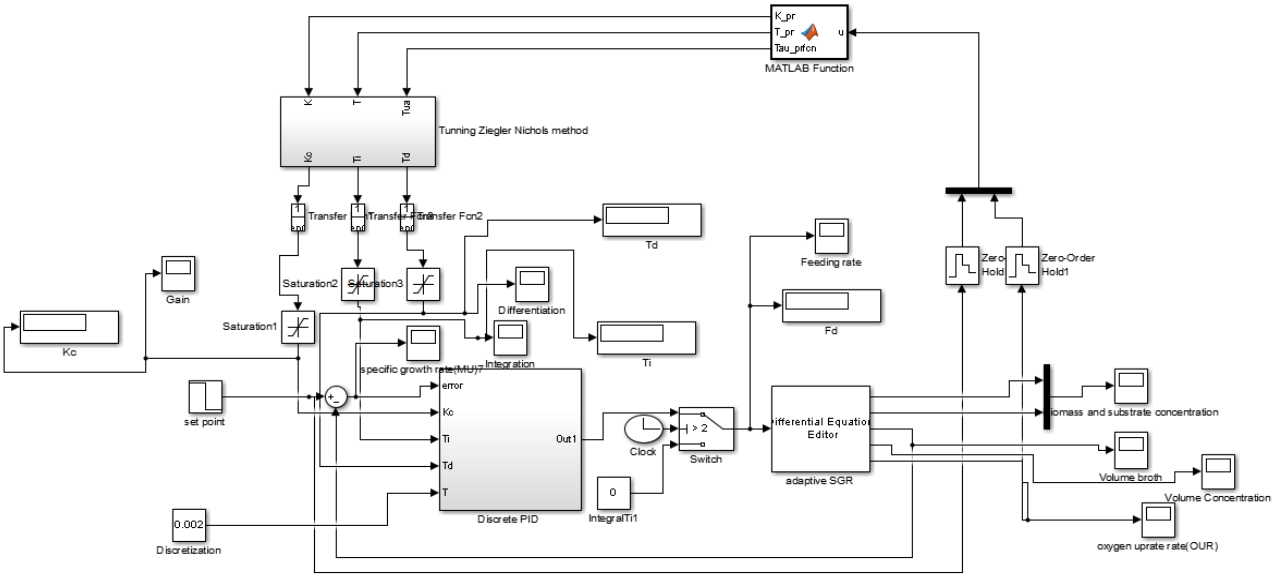

Number 15. Discrete PID controller design

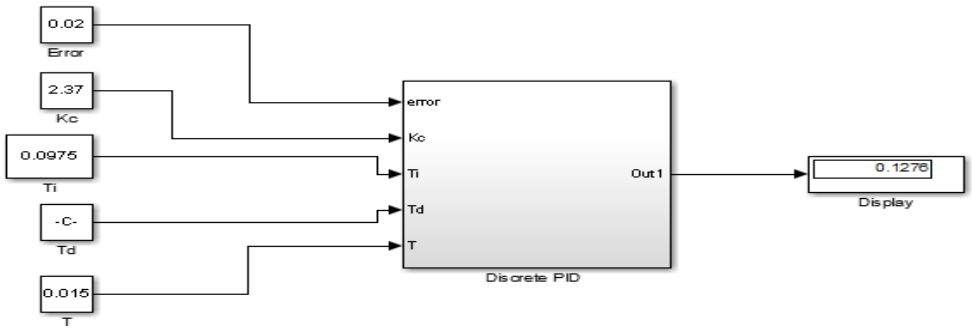

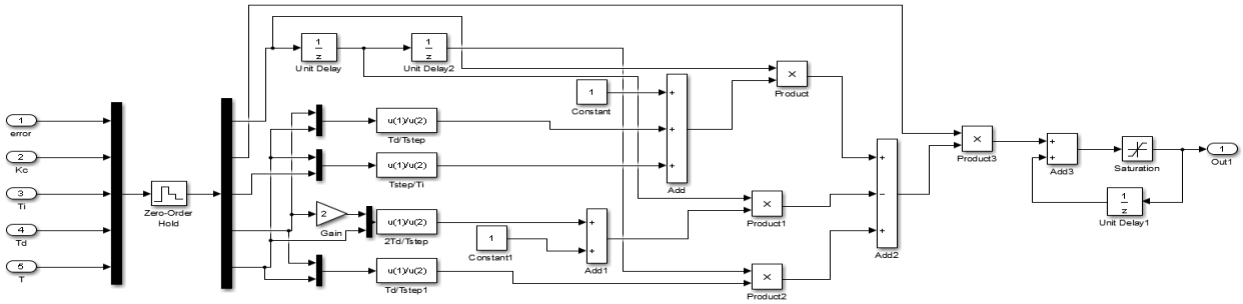

Number 16. External noise

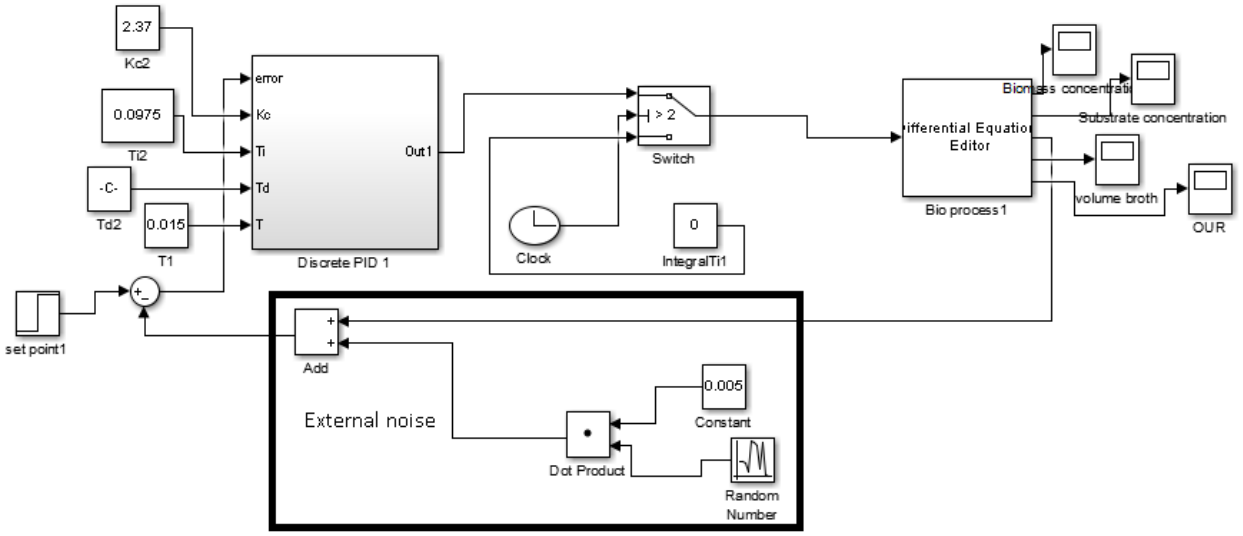

Number 17. The comparison performance indices of the adaptive and the ordinary control systems